

✓

The Nottingham Trent University
Library & Information Services
SHORT LOAN COLLECTION

Date	Time	Date	Time

Please return this item to the Issuing Library.
Fines are payable for late return.

THIS ITEM MAY NOT BE RENEWED

Short Loan Coll May 1996

40 0681760 X



ProQuest Number: 10290064

All rights reserved

INFORMATION TO ALL USERS

The quality of this reproduction is dependent upon the quality of the copy submitted.

In the unlikely event that the author did not send a complete manuscript and there are missing pages, these will be noted. Also, if material had to be removed, a note will indicate the deletion.



ProQuest 10290064

Published by ProQuest LLC (2017). Copyright of the Dissertation is held by the Author.

All rights reserved.

This work is protected against unauthorized copying under Title 17, United States Code
Microform Edition © ProQuest LLC.

ProQuest LLC.
789 East Eisenhower Parkway
P.O. Box 1346
Ann Arbor, MI 48106 – 1346

~~1-1-13~~

Emph 1.

ELECTRONIC INSTRUMENTATION FOR PARTICLE MASS
FLOW RATES IN PIPES

Mohamed LASHAB (D.E.S. in physics)

Thesis submitted to the Council for National Academic
Awards for the degree of
Master of Philosophy

Department of Electrical and
Electronic Engineering
Trent Polytechnic
Nottingham

Collaborating Establishment:
CEGB,
Kelvin Avenue,
Leatherhead,
Surrey.

November 1988

Acknowledgements

I would like to express my deep thanks to Dr B.C O'Neill my supervisor for his patient help, advice, and support throughout the project. I would like to thank Dr R.W.J Barker for his revision to the thesis especially the electronics part.

Many thanks to E.Mills, S.Clark and P.Evison for their friendship and unfailing support.

My appreciation also goes to Dr P.Holmes head of department, for his help and support.

Finally I would like to thank all the technicians for their help, specially D.Antcliff, R.Ash and M.Saywell for transferring my files to the MicroVAX and printing out this thesis.

ABSTRACT

The aim of the project is to measure the mass flow rate of an electrostatic spraying process, by means of a novel pulse charge technique. This involves three main topics. First the study of the physical process of charging and collection. Second the design of charge detection electronic instrument. Finally the measurement and analysis of the experimental data in order to predict the flow rate.

The study of the physical process of charging and collection involved the examination of the charge injection and corona discharge, and the study of charge collection to optimize the sensor length and the charge injection pulse width.

The charge detection electronic instrument measures the charge induced at the sensors. Due to the low magnitude of the charge detected, circuit analysis was necessary to minimize the electrical noise in the devices.

The experimental work consists of interfacing the electronic instrument designed, to the microcomputer system for data analysis. Data was collected over a wide range of parameter variation, and it was possible with the microcomputer system to perform statistical analysis on this data. The result showed that there was a wide range of fluctuation in the original data but with analysis it was possible to obtain an accurate prediction of the flow rate from the sensor.

CONTENTS

	<u>Page</u>
Chapter one	
<u>INTRODUCTION</u>	
1.1 Mass flow rate measurement	1
1.2.1 Capacitance noise	
1.2.2 Pulse charge injection	
1.2 Electronic instrument	3
1.3.1 Input stage and noise	
1.3.2 Signal processing	
1.3 Thesis structure	4
Chapter two	
<u>THEORY OF CHARGED PARTICLES</u>	
2.1 Introduction	6
2.2 Corona discharge	6
2.3 Electric field at the walls	7
2.3.1 Case of point charge	7
2.3.2 Case of line charge	9
2.4 Charge collected at the sensors	13
2.4.1 Flux due to a point charge	13
2.4.2 Flux due to a line charge	16
2.5 Singals induced at the sensors	23
Chapter three	
<u>SIGNAL PROCESSING</u>	
3.1 Introduction	25
3.2 Signal processing	25
3.2.1 Peak detector	27
3.2.2 Sample and hold	27
3.3 Circuit analysis	29

3.3.1 Current to voltage converter	31
3.3.2 Integrators	34
3.4 Noise analysis	36
3.4.1 Basic noise properties	36
3.4.2 Signal to noise ratio	37
3.5 Test on the electronic system	

Chapter four

INTERFACE WITH THE MICROMPUTER

4.1 Introduction	41
4.2 Hardware	41
4.2.1 User port of BBC	43
4.2.2 A to D converter	43
4.3 Software	45
4.3.1 Main program	45
4.3.2 Data processing	47

Chapter five

EXPERIMENT AND RESULTS

5.1 Introduction	48
5.2 Experimental procedure	48
5.2.1 Pneumatic system	48
5.2.2 High voltage power supply	50
5.3 Data processing	51
5.3.1 Mean absolute deviation	53
5.3.2 Standard deviation	53
5.4 Results and discussion	53
5.4.1 Comment on Q1, Q2, Q3.	54
5.4.2 Ratio Q2/Q1	54
5.5 Conclusion	58

Chapter six

CONCLUSION AND FURTHER WORK

6.1 Conclusion	61
----------------	----

6.2 Further work	61
6.2.1 Powder control	62
6.2.2 High voltage pulse generator	63
6.2.3 Electrostatic precipitators	64

References

- Appendix A : Poinsson's solution for point charge in grounded cylinder.
- Appendix B : Circuit analysis for a current to voltage converter and an integrator.
- Appendix C : Programs in FORTRAN of electric feild and electric flux analysis.
- Appendix D : Programs in BASIC of Mass flow rate measurement record and data analysis.
- Appendix E : 6809 software listing of powder flow control.

FIGURES

	<u>Page</u>
1.1 Pulse charge injection method.....	5
2.1 Electrostatic charging process.....	7
2.2 Ideal point charge or line charge.....	9
2.3 Bessel function solution routine.....	10
2.4 Electric flux density case of point charge.....	11
2.5 Electric flux density case of line charge.....	14
2.6.a Flux enclosed case of point charge.....	17
2.6.b Comparison between parallel plates and a cylinder	17
2.7 Flux enclosed case of variable line charge.....	19
2.8 Charge sensed case of line charge, variable pulse..	21
2.9 Charge sensed case of line charge, variable sensor.	22
3.1 Circuit diagram of the analog circuit.....	26
3.2 Integrator and peak detector.....	28
3.3.a Sample and hold.....	30
3.3.b Timing diagram of the signal processing.....	29
3.4 Equivalent current source	32
3.5 Current to voltage converter and amplifier.....	33
3.6 Linearity of the analog circuit.....	36
4.1 Circuit diagram of the interface.....	42
4.2.a User port of the BBC.....	44
4.2.b A to D converter, interface with the BBC.....	44
4.2.c Timing diagram of the A to D converter.....	43
4.3 Flow chart of the data analysis.....	46
5.1 BBC ucp interface with the pneumatic system.....	49
5.2 Signal delivered by the sensors.....	52
5.3 Data record of Q2/Q1 with respect to MFR.....	55
5.4-5 Data analysis of Q2/Q1.....	56-7
5.6-7 Standard deviation on the ratio Q2/Q1.....	59-60
6.1 Flow chart of a mass flow rate regularisation.....	65

LIST OF SYMBOLES

q is an elementary charge
 s sensor length
 e potential
 L line charge length
 ϵ dielectric permittivity
 D electric density of the flux
 Q total charge collected
 S standard deviation
MFR mass flow rate
ADC analog to digital converter
S/H sample and hold
 Z_{inl} open loop input impedance
 Z_{incl} closed loop input impedance
 J_1, J_0 Bessel functions
op-amp operational amplifier
SNR signal to noise ratio
 V_{io} input offset voltage
 I_{io} input offset current
 I_b bias current
MAD

Chapter 1

INTRODUCTION

Electrostatic powder coating is a widely used technique in the painting industry, and has many advantages over the other processes. Powder painting is more economical than solvent based paints. It uses less energy to dry/fuse the paint, and any powder missing the target can be recycled. The main parameters that determine the finish are mass flow rate and the time taken to coat the object. A secondary parameter of the coating process control is the back ionization, based on the particle size and resistivity of the powder, which means that extra powder coming is neutralized by ions from the layer. In fact this is one of the advantages of this process known as self-limiting effect of the paint.

In an industrial painting process, the powder is transported from the hopper to the object by means of pneumatic conveyance and it is charged by a high voltage corona discharge at the tip of the spray gun. The coated object is placed into an oven at an appropriate temperature, where the powder particles fuse and the painting is finished.

The aim of the project is based on three parts. Firstly to optimize the sensors and the pulse charge length, this involves Laplace's solution applied to the electrostatic problem. Secondly is to develop an instrument capable of measuring the mass flow rate of particles in ducting, over a small cross-sectional area. Finally is to interface the instrument to a microcomputer in order to analyse the correlation of the measured mass flow rate and the predicted one.

To measure the mass flow rate, the project uses a pulse charging technique. A pulse of charge is injected into the

powder/air stream via a corona needle located along the axis of the pipe of the detector. Charged powder is carried downstream in the pipe, where sensors are located.

1.1 Mass flow rate measurement

The control of particulate processes cannot be satisfied unless the measuring techniques have been developed. Powder flow rate measurement in gas-solid two phase flow is a complicated and a critical process, since the variables of state of both gas and solid are independent and may vary widely. There are several techniques for measuring the powder flow rates in pipes, three of which are optical/microwave, capacitance noise and pulse charging.

1.1.1 Optical/Microwave method

Optical and microwave method: MALYSHEV [4] When particles interrupt two separate optical/microwave beams, the time of flight between the two beams determines the velocity of the powder. For mass flow rate measurement, a single beam of laser light is crossed and the frequency of the beam changes. This is known as doppler effect. This technique is not suitable for the small size of particles and small pipe diameters normally used in powder spraying.

1.1.2 Capacitance noise method

The capacitance noise technique GREEN [2] is based on the principle that a change in density of powder changes the capacitance of the transducer forming part of the pipe's wall, because the dielectric of the capacitor is proportional to the density of the powder. By measuring the capacitance of the transducer the mass flow rate can be obtained.

In practice it is difficult to obtain an absolute value of the capacitance, this is due to the continuous build up of powder on the wall of the pipe. The capacitance also depends

on other parameters other than the mass flow rate, which make it unreliable. BECK [3]

1.1.3 Pulse charge injection method

Pulse charge injection method, which was developed in this laboratory, consists of charging the powder flowing in the pipe, using a high voltage power supply. The pulse is at a voltage of 6KV, for a duration of, 5ms and is at low energy level. Four sensors located along the pipe, detect the charge induced at the walls of the pipe.

Charge detection is obtained by using current amplifiers and integrators. Due to the time delay between the signals, these are processed by an analog signal processing unit, in order to give a simultaneous reading.

1.2 Electronic instrument

WILLIS [1] used a technique of peak current detection to measure the flow rate. In this project a method of charge detection was used. The two methods were then compared for accuracy and efficiency of use.

Because of the small size of the current that the charge induces in the sensors, FET op-amps were chosen because of their high impedance, and low input bias current. When injecting a pulse charge inside the pipe, sensors located in the pipe, detect the charge with a differing time delay due to their position. This time difference is overcome by the use of peak detector and sample and hold circuitry.

1.3 Thesis structure

This thesis contains four main parts, each part is treated in a separate chapter with greater detail. Chapter two deals with the charging process and the study of the charge induced by the sensors which determines the design of the sensors,

that are connected to the measurement device. Chapter three contains the circuit analysis and signal processing used in the electronic instrument. The instrument is then used in chapter four to interface with the BBC microcomputer, in order to analyse the parameter which predict the flow (its correlation with the mass flow rate). The latter involves a lot of statistics. Finally, chapter five, describes the experimental procedure, and discusses the results obtained.

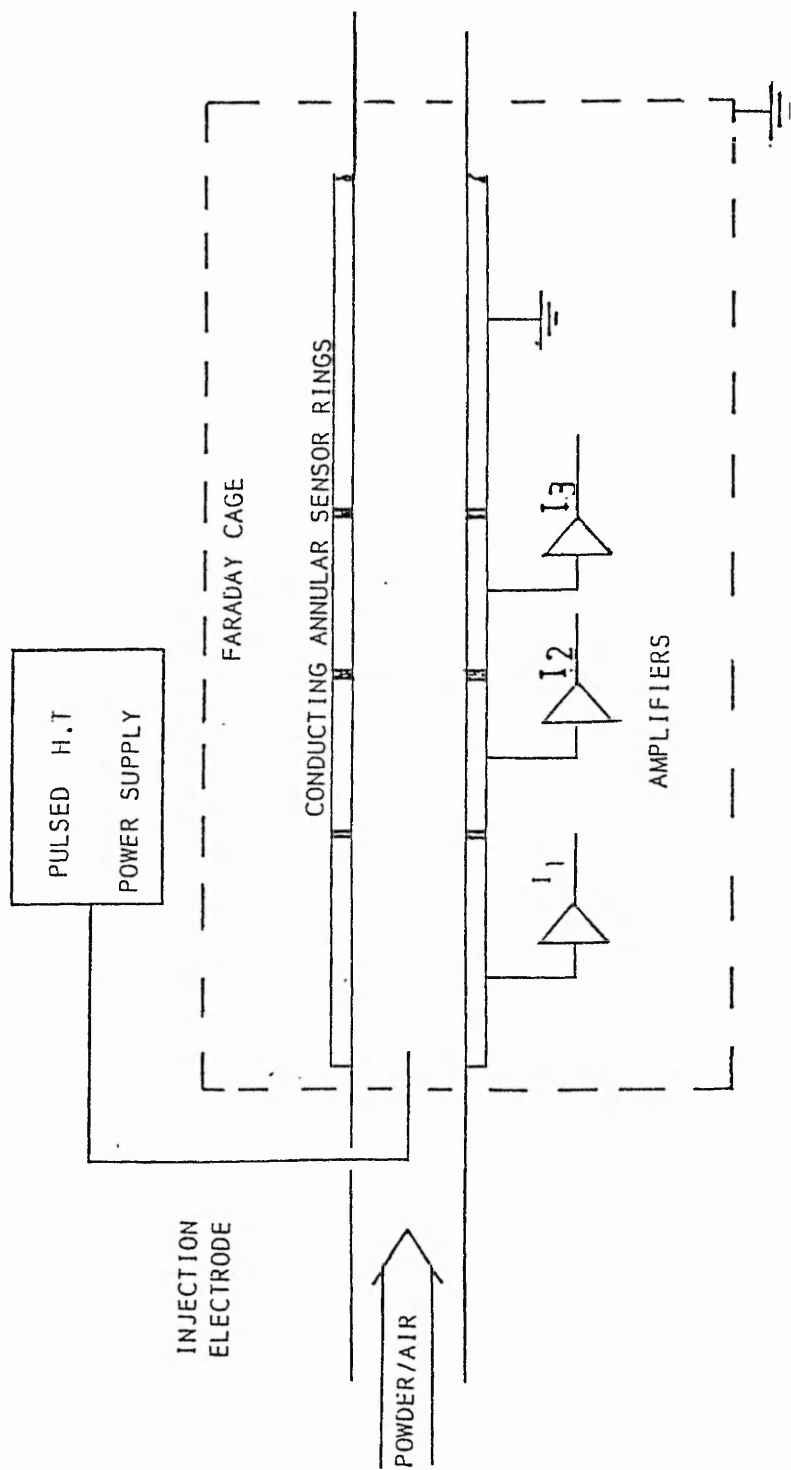


Fig 1.1

Pulse charge injection method, schematic view

Chapter 2

THEORY OF CHARGED PARTICLES

2.1 Introduction

In an electrostatic powder coating process, the powder is charged by a high voltage needle, using an H.T pulse generator. The electric field is very intense round the needle at which corona discharges, hence particles are charged by ion bombardment. Powder carried down-stream, sticks at the grounded walls of the pipe, where sensors are located, and generates an electric current. This chapter is concerned with the charging process of the powder, (the corona discharge), and the charge detection.

The charge induced in the sensors is obtained by a study of the flux lines, which can be calculated by applying Poisson's equation to a point charge inside a cylinder. From this study, the performance of the flow of an ideal charge particle along the centre of the pipe can be obtained for various sensor lengths, hence an optimum sensor length can be determined. Also the signals delivered by the sensors can be predicted.

2.2 Corona discharge

The corona discharge is defined as the leakage of the charge brought about by the ionization of the air surrounding the needle, break-down of the air in the immediate vicinity of the point occurs only at very high voltage.

The project uses a positive corona discharge, which is caused by a positive potential applied at the needle in Fig (2.1). A value of potential will be reached at which the needle begins to discharge itself to the surrounding air via the sharp point of the needle. Powder is charged by positive

ions (free ions) travelling towards the collector.

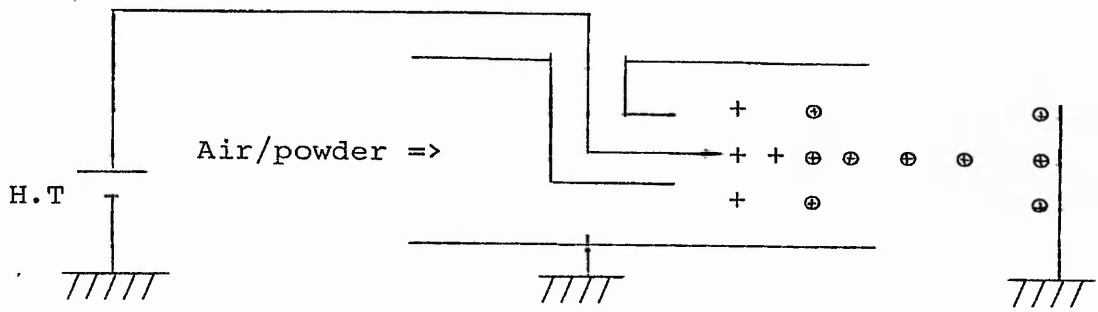


Fig 2.1

2.3 Electric field

The electric field analysis is based on Poisson's solution for a point charge or a line charge, which does not take into account the effect of space charge on the electric field distribution. Also the needle axis is assumed to be in free space, which means that needle is considered to be a point charge. The potential given by Poisson's solution in appendix A is:

$$\Phi = \frac{q}{2\pi\epsilon_0 r_0^2} \sum_{l=1}^{\infty} \exp(-k_l |z|) \frac{J_0(k_l r)}{k_l [J_1(k_l r_0)]^2} \quad (2.1)$$

Where J_0 , and J_1 are Bessels functions, and k the ensemble of solutions. The electric flux density is obtained first, by using a master solution based on a point charge inside a cylinder, then this is extended to a line charge.

2.3.1 Case of a point charge

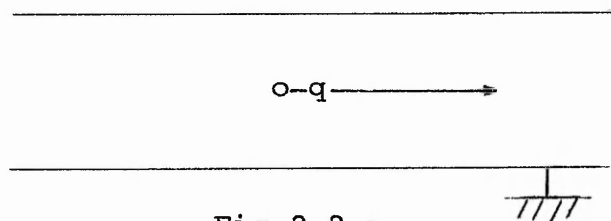


Fig 2.2.a

The ideal problem illustrated by Fig (2.2.a), makes it easy to find the electric field induced at the walls of the pipe, by only a point charge inside a cylinder . From Maxwells equation, the electric field is

$$E = - \text{grad}(\Phi)$$

Now using the above equation, the electric field inside the cylinder is equal to

$$E_z = - \frac{\partial \Phi}{\partial z}, \quad E_r = - \frac{\partial \Phi}{\partial r} \quad (2.2)$$

Where E_z is the axial component, and E_r is the radial component. Using the electric field of (2.1), the new components are

$$E_z = \frac{q}{2\pi\epsilon_0 r_0^2} \sum_{l=1}^{\infty} k_l \exp(-k_l |z|) \frac{J_0(k_l r)}{k_l [J_1(k_l r_0)]^2} \quad (2.3)$$

$$E_r = - \frac{q}{2\pi\epsilon_0 r_0^2} \sum_{l=1}^{\infty} \exp(-k_l |z|) \frac{1}{k_l [J_1(k_l r_0)]^2} \frac{\partial J_0(k_l r)}{\partial r} \quad (2.4)$$

Which make the first component $E_z = 0$ at $r = r_0$, because $J_0(r_0) = 0$. While the second component E_r depends on the value of $J_0'(r)$. Using one of Bessels equations

$$\frac{dJ_n(x)}{dx} = n \frac{J_n}{x} - J_{n+1}$$

Hence

$$\frac{dJ(k_l r)}{dr} = -k_l J_1(k_l r) \quad (2.5)$$

Putting (2.5) in (2.4) gives

$$E_r = \frac{q}{2\pi\epsilon_0 r_0^2} \sum_{l=1}^{\infty} \exp(-k_l |z|) \frac{1}{J_1(k_l r_0)} \quad (2.6)$$

Let $a = k r_0$, which is the solution of $J_0(k r_0) = 0$, and let

$$CJ(a) = \frac{1}{J_1(a)} , \quad D_0 = \frac{q}{2 \pi r_0^2}$$

When using (2.6), the electric flux density becomes equal to

$$D_r = D_0 \sum_a CJ(a) \exp(-|z| \frac{a}{r_0}) \quad (2.7)$$

The expression (2.7) is deliberately written in such way as to make it easy to compute, yet the series needs hundreds of terms, involving Bessel function solutions $J_0(a)=0$, especially near $z = 0$. Software in appendix C, based on the numerical solution, was written to sum these terms. Fig 2.3 shows the Bessel function solution $J_0(a) = 0$ routine.

The value (D_r / D_0) was found to be equal to 0.664 near $z = 0$. The electric flux density induced at the walls of the pipe in Fig (2.4), shows how the distribution varies with respect to z .

2.3.2 Case of a line charge

By assuming a perfect pulse of charge, a uniform line charge will be created along the centre of the pipe. The length of the line will depend on the duration of the pulse and the velocity of the powder. Fig (2.2.b) shows a line charge of length L , inside a grounded cylinder. The previous case of a point charge is extended to line charge, where a series of points are simulated to a line charge.

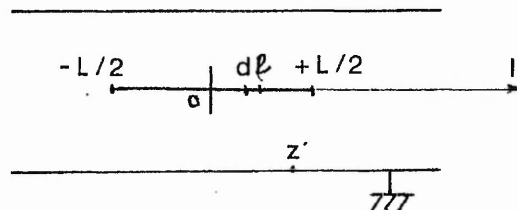


Fig 2.2.b

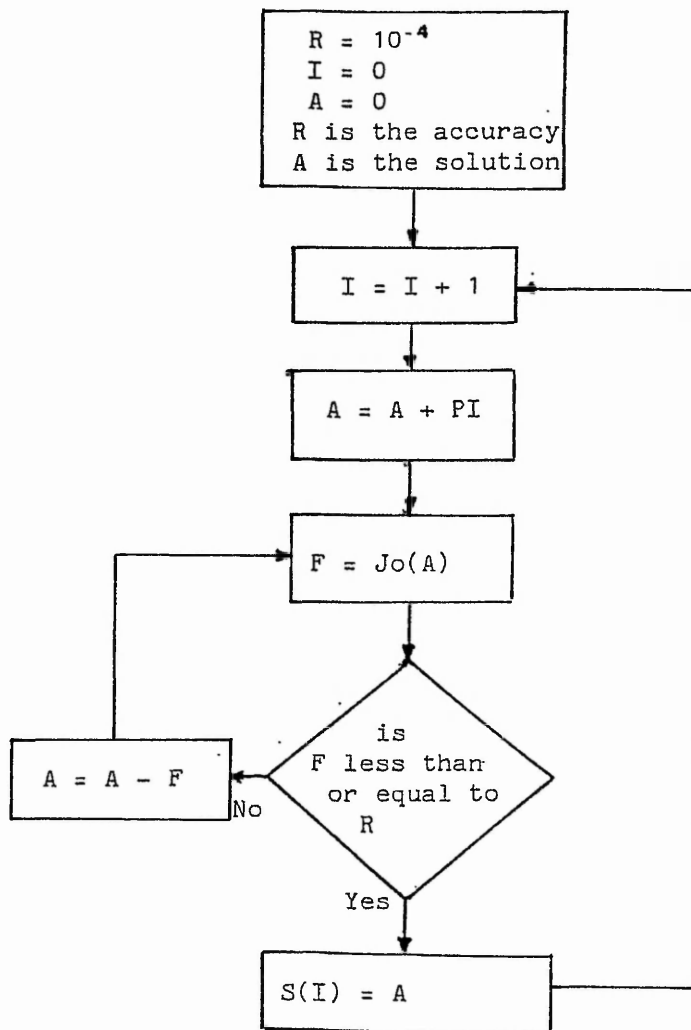


Fig 2.3

Bessel function solution routine

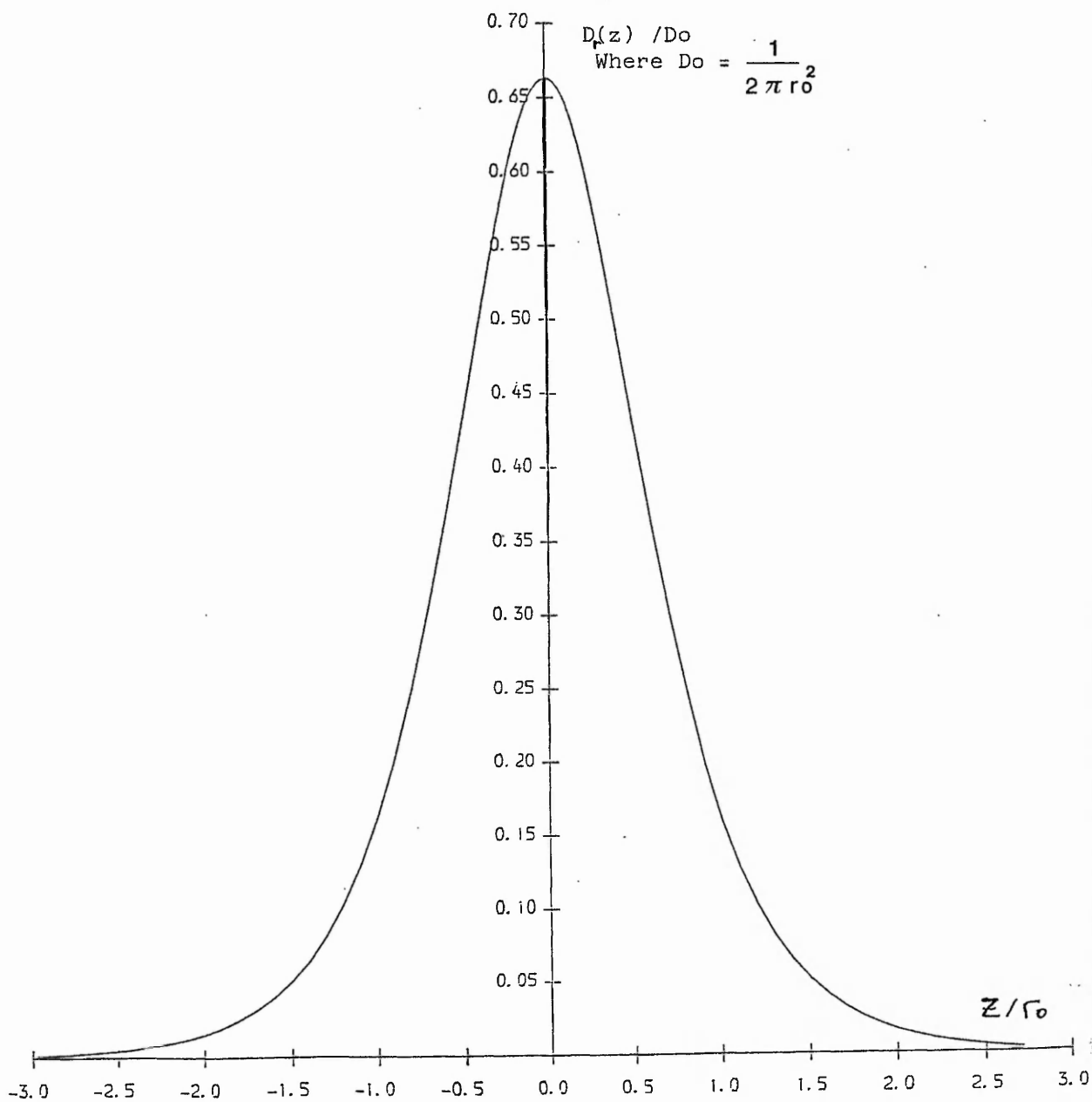


Fig 2.4

Electric flux density sensed at the walls of the pipe, case of a point charge

The electric field calculation based on the previous section, can be obtained by making.

$$q = \lambda.L \quad dq = \lambda.d\ell \quad (2.8)$$

Where λ is the linear density of charge, and dq is an elementary point charge. Suppose z' is the place at which we are looking for the electric field. Here two cases are presented.

a) Case of $|z'| > L/2$, using the master solution for a point charge (2.6), the electric field at z' is the sum of several point charges one after the other. An elementary charge dq produces an electric field

$$dD(z') = \frac{dq}{2\pi r_0^2} \sum_a CJ(a) \exp(-\frac{|z'-\ell|}{r_0} a) \quad (2.9)$$

Hence the total density of charge is

$$D(z) = D_0 \sum_a \lambda \int_{-L/2}^{+L/2} CJ(a) \exp(-\frac{|z'-\ell|}{r_0} a) d\ell \quad (2.10)$$

Where $D_0 = \frac{1}{2\pi r_0^2}$, after integration, all calculus done

$$D(z) = D_0 \sum_a \frac{2r_0}{La} \frac{1}{J_1(a)} \exp(-\frac{|z|}{r_0} a) \sinh(\frac{L}{2r_0} a) \quad (2.11)$$

b) Case of $|z'| < L/2$, here the electric field is symmetrical at $z = z'$

$$D(z) = D_0 \sum_a \frac{1}{L J_1(a)} \left(\int_{z'}^{L/2} \exp(\frac{z'-\ell}{r_0} a) d\ell + \int_{-L/2}^{z'} \exp(-\frac{z'-\ell}{r_0} a) d\ell \right)$$

After integration

$$D(z) = D_0 \sum_a \frac{2r_0}{La} \frac{1}{J_1(a)} \left[1 - \exp\left(-\frac{L}{2r_0} a\right) \cosh\left(\frac{z'}{r_0} a\right) \right] \quad (2.12)$$

The graph of Fig (2.5) shows the electric flux density for a line charge of *different* lengths with respect to z , which gives the two expressions obtained (2.11) and (2.12) in one graph. Here it can be seen that for a small line ($L = 0.14\text{mm}$) the graph is similar to the one obtained for a point charge. It is important to notice that for a bigger value of pulse length, the electric field is almost constant nearby the charge.

2.4 Charge collected at the sensors

In this section there is need to optimize the sensor length, because it is important to have a very long sensor which encloses the maximum flux, at the same time the loss of charge between sensors suggests a short length, therefore a compromise is necessary.

To find the charge collected by a sensor of length s , it is useful to use the expression of electric flux density, and Maxwells equation (2.13)

$$\int_{-\infty}^{+\infty} D_r(z) \cdot ds = q \quad \text{let say } q = 1 \quad (2.13)$$

By making the charge unity, $q = 1$, it means that the total charge induced inside a sensor is less than one. In the next sections the charge calculated is given as a percentage of the total charge.

2.4.1 Master solution

The sensor is located at $z = z'$, where z' is a variable. Here the charge sensed at the sensors, is due to electric field given by (2.7).

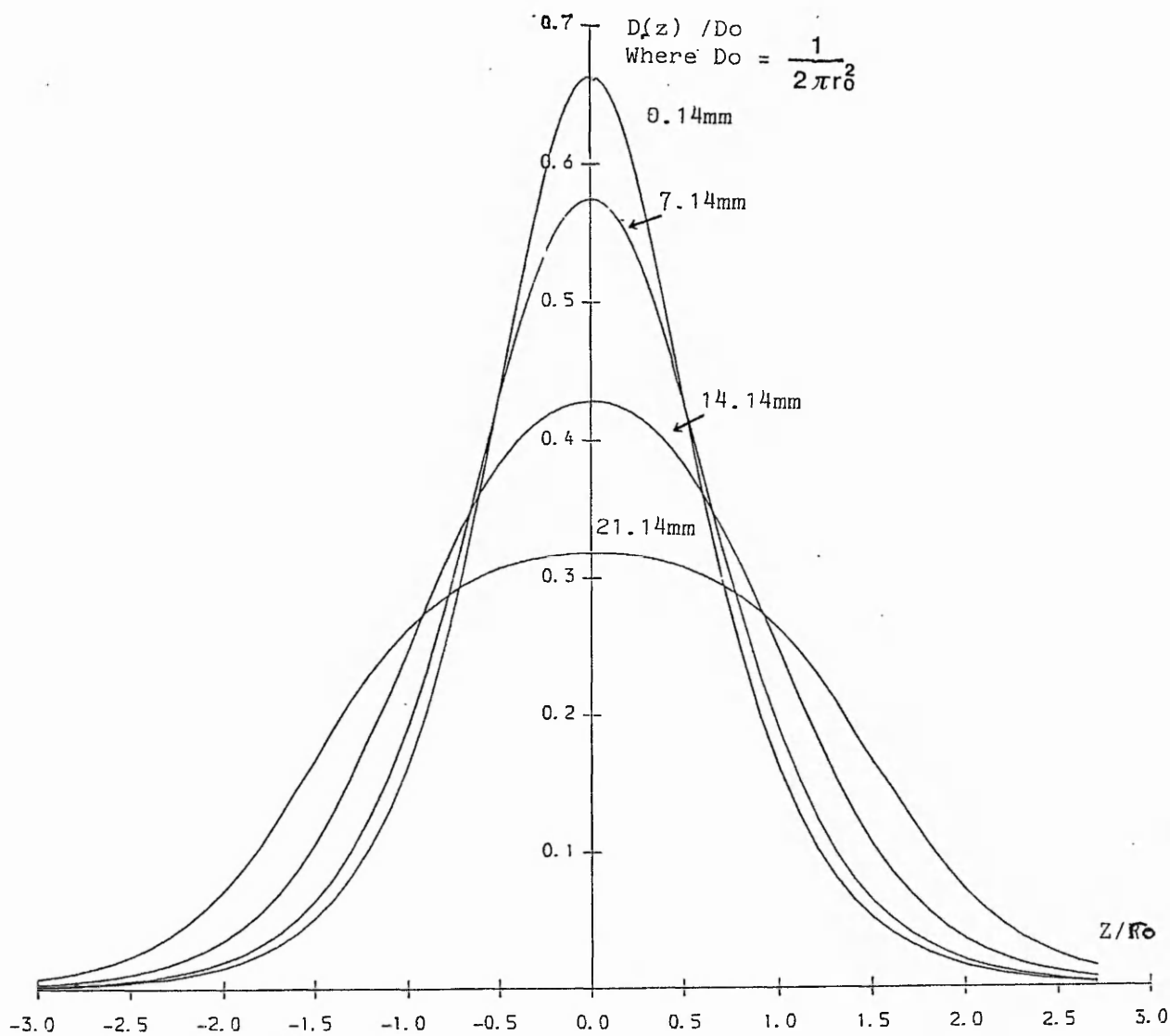


Fig 2.5

Electric flux density induced at the walls of the pipe
case of a line charge

a) Case of $|z'| < s/2$, using equation (2.13) and (2.7), the charge collected is

$$2 \pi r o \int_{z1}^{z2} D r(z) dz = D o \sum_a C J(a) \left(\int_{z'-s/2}^0 \exp(z a/r o) dz + \int_0^{z'+s/2} \exp(-z a/r o) dz \right) \quad (2.14)$$

$$Q = D o 2 \pi r o \sum_a \frac{r o}{a J_1(a)} (1 - \exp((z'-s/2) a/r o) + 1 - \exp(-(z'+s/2) a/r o))$$

Finally

$$Q = \sum_a \frac{2}{a J_1(a)} [(1 - \exp(-s a/2 r o) \cosh(z' a/r o))] \quad (2.15)$$

b) Case of $|z'| > s/2$, here the electric field can be obtained by simply using the same process.

$$Q = 2 \pi r o \int_{z1}^{z2} D r(z) dz = D o \sum_a \frac{2 \pi r o}{J_1(a)} \int_{z1}^{z2} \exp(-|z| a/r o) dz$$

All calculus done the final expression is

$$Q = \sum_a \frac{2}{a J_1(a)} \exp(-|z| a/r o) \sinh(s a/2 r o) \quad (2.16)$$

Both (2.15) and (2.16) have charge dimension ,the only problem in computing these equations is the solution of $J_0(A) = 0$. When making $z = 0$, it follows that.

$$Q = \sum_a \frac{2}{a J_1(a)} [1 - \exp(-s a/2 r o)] \quad (2.17)$$

The plot of (2.17) in Fig 2.6, shows that the flux enclosed is proportional to the sensor length, when the length is relatively small compared to the diameter of the pipe. When the sensor length is much greater than the radius, the flux enclosed reaches 100 % of the total flux. The graph also shows that for a sensor length of 21mm the flux reaches 95 % of the total flux. This means that the sensor is close to the ideal.

The comparison between this model and the approximate parallel plate model used by Willis [2.1] is shown in Fig 2.6.b, which shows the error obtained by Willis in assuming a parallel plate model of the flow.

2.4.2 Flux due to a line charge

The flux induced in the sensors due to the line charge is obtained by the superposition of the result of point charges displaced at small intervals along the length of the line charge and integrating the result. Fig 2.2.c shows a line charge of length L inside a cylinder and a sensor of length s . The solution presents different cases, whether $L > s$, or $s > L$.

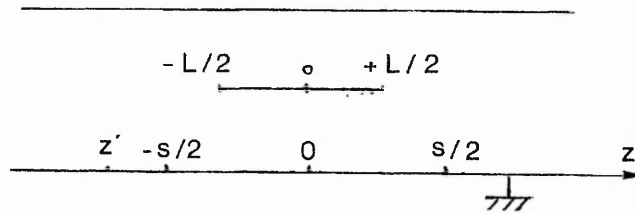


Fig 2.2.c

a) Case of $|z'| < |L-s|/2$ in Fig 2.2.c, using Maxwells equation (2.13) and the electric flux density of (2.12), it follows that

$$Q = 2\pi \int_{z_1}^{z_2} r_0 D(z) dz$$

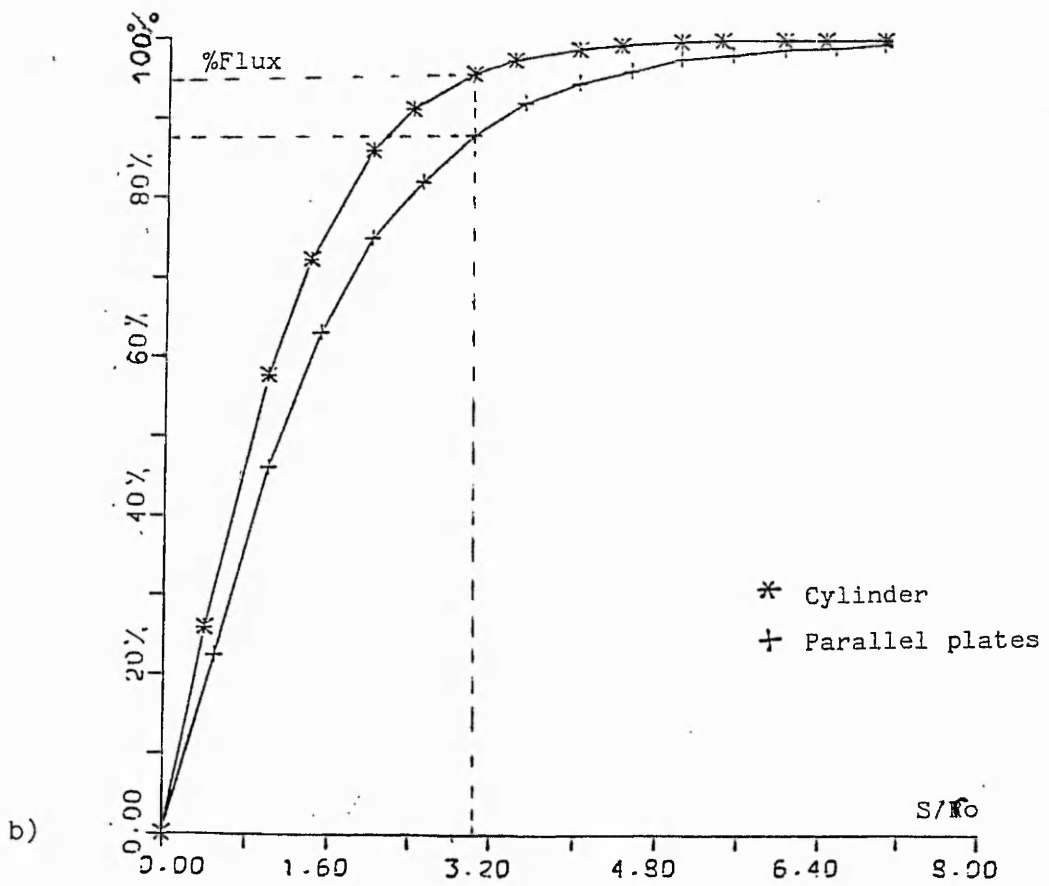
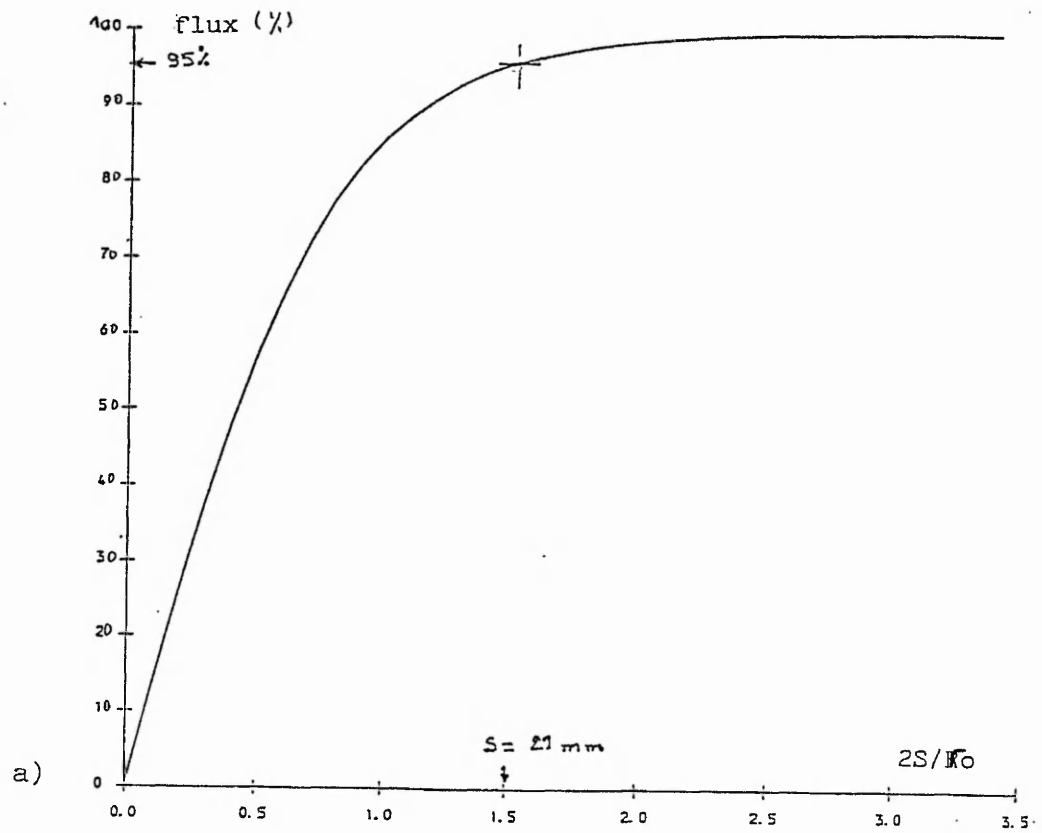


Fig 2.6

- a) Flux enclosed inside a cylinder due to a point charge
 b) Comparison between parallel plate and cylindrical models

$$Q = D_0 \sum_a \frac{4\pi r_0^2}{a J_1(a)} \int_{z'-s/2}^{z'+s/2} [(1 - \exp(-aL/2r_0) \cosh(az/r_0))] dz$$

Thus

$$Q = \sum_a \frac{2}{a J_1(a)} \left(\frac{s}{L} - \frac{2r_0}{aL} \exp(-as/2r_0) \sinh(aL/2r_0) \cosh(za/r_0) \right) \quad (2.19)$$

The case of s less than L can be obtained in the same manner by just replacing s by L .

When making $z = 0$ at (2.19) this becomes equal to

$$Q = \sum_a \frac{2}{a J_1(a)} \left[1 - \frac{2r_0}{aL} \exp\left(-\frac{as}{2r_0}\right) \sinh\left(\frac{aL}{2r_0}\right) \right] \quad (2.20)$$

The graph of (2.20) in Fig 2.7, shows the flux enclosed at different values of l , as function of s . When making $l = 0$ in (2.19), which is the case of a point charge, this becomes equal to

$$Q = \sum_a \frac{2}{a J_1(a)} [1 - \exp(-sa/2r_0)]$$

This is equivalent to (2.17). Another way to check the calculus error, is to see if there is a continuity of the flux $Q(z)$ in the different cases of z , $(s-L)$ and $(s+L)$.

b) Case of $(L+s)/2 > |z'| > |L-s|/2$ in Fig 2.2.c, here the charge is the sum of the charges induced by the density of flux (2.11) and (2.12)

$$Q = D_0 \sum_a \frac{4\pi r_0^2}{a J_1(a)} \int_{z'-s/2}^{+L/2} (1 - \exp(aL/2r_0) \cosh(az/r_0)) dz + \int_{+L/2}^{z'+s/2} \exp(az/r_0) \sinh(aL/2r_0) dz$$

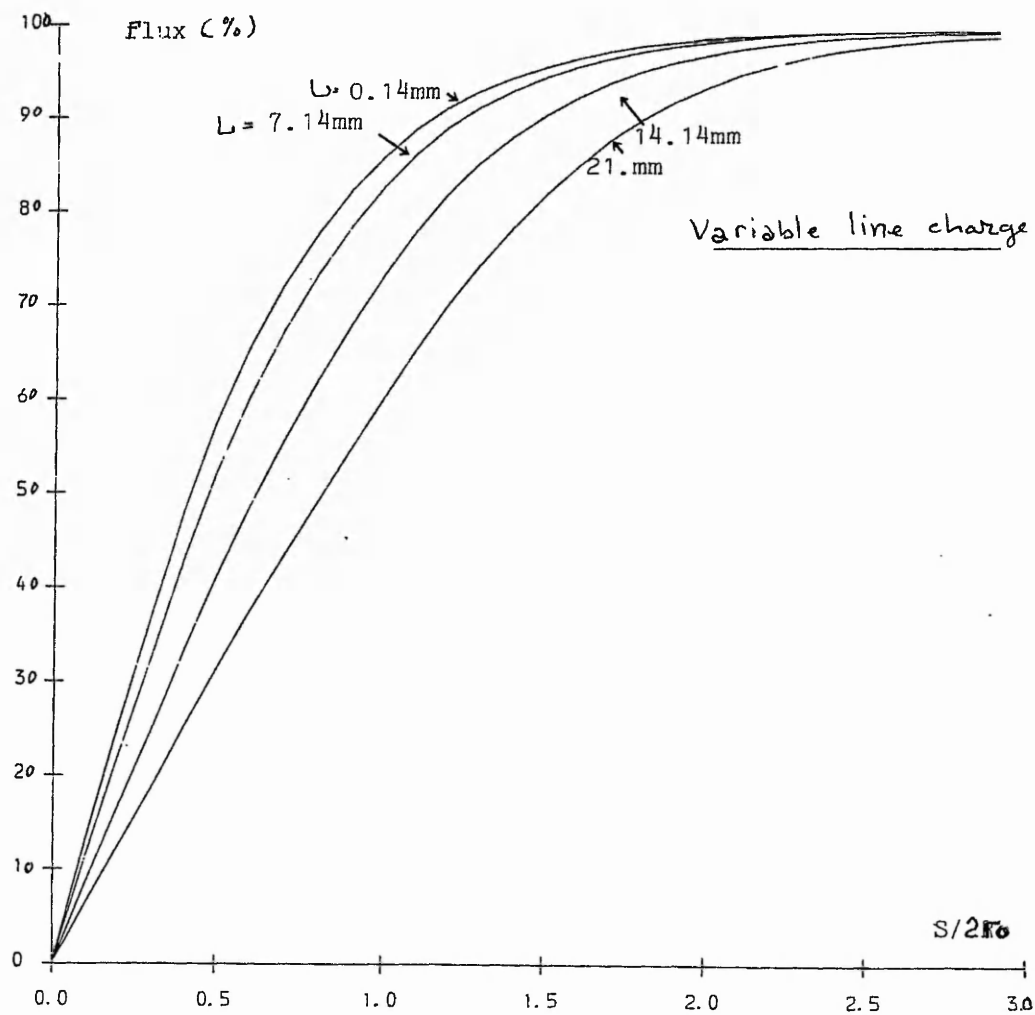


Fig 2.7
Flux enclosed inside a sensor S , case of a line charge

Therefore

$$Q = \sum_a \frac{2}{a J_1(a)} \left[\frac{L+s}{2L} - \frac{z'}{L} + \frac{r_0}{aL} \left\{ \cosh(az/r_0) \exp\left(-\frac{L+s}{2r_0} a\right) - \cosh\left(a \frac{L-s}{2r_0}\right) \exp\left(-\frac{|z'|}{r_0} a\right) \right\} \right] \quad (2.21)$$

c) Case of $|z'| > (L+s)/2$ in Fig 2.2.c , here the electric field is given by (2.11), therefore the charge collected is

$$Q = D_0 \sum_a \frac{4\pi r_0^2}{L a J_1(a)} \int_{z'-s/2}^{z'+s/2} \sinh(al/2r_0) \exp\left(-\frac{|z'|}{r_0} a\right) dz \quad (2.22)$$

After integration

$$Q = \sum_a \frac{2}{a L J_1(a)} \left(\frac{r_0}{a} \right) \sinh\left(a \frac{L}{2r_0}\right) \left[\exp\left(-\frac{a}{r_0} (z' + s/2)\right) - \exp\left(-\frac{a}{r_0} (z' - s/2)\right) \right]$$

Finally

$$Q = \sum_a \frac{1}{L J_1(a)} \frac{4r_0}{a^2} \sinh(as/2r_0) \sinh(al/2r_0) \exp\left(-\frac{|z'|}{r_0} a\right) \quad (2.23)$$

Now the charge sensed inside a sensor of length s , due to a travelling line charge of length L , can be obtained by gathering the three equations (2.19), (2.21) and (2.23). The graph of Fig 2.8 shows the percentage of charge sensed, due to a pulse charge of $L=21\text{mm}$ with various values of sensor length. Whereas Fig 2.9 shows the percentage charge sensed at sensor of length $s=21\text{mm}$, due to variable pulse length.

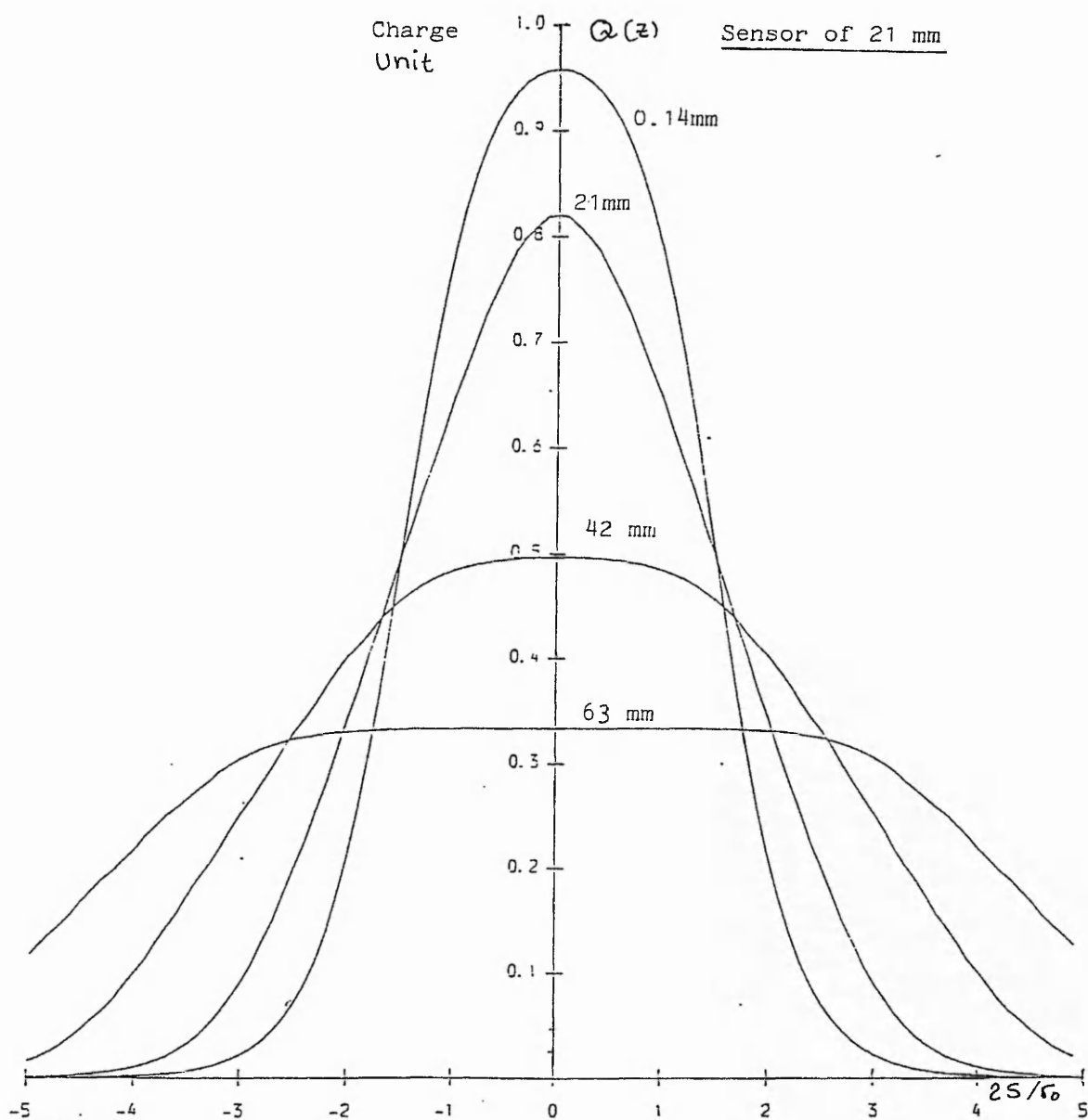


Fig 2.8

Charge collected inside a sensor of 21 mm length. due to a variable line charge

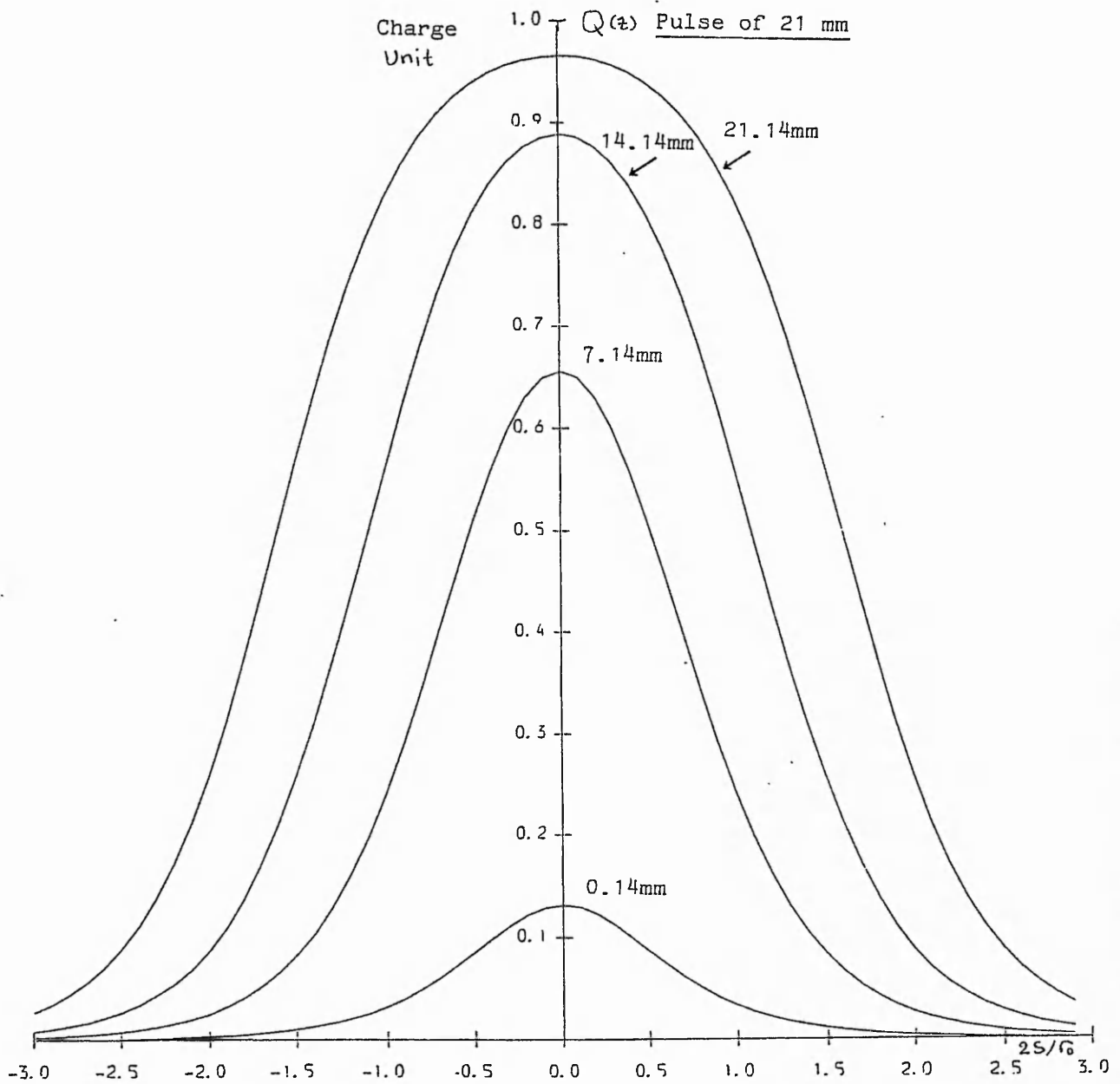


Fig 2.9

Charge collected inside a sensor of variable length, due to a line charge of 21mm

The sensors and pulse charge are chosen to enable large flux detection and low loss of charge, thus these are given the values of $s=21\text{mm}$ and $L=21\text{mm}$, where the charge sensed is more than 80 %, which is close to the ideal.

2.5 Signal induced at the sensors

The previous section dealt with pulse charge and sensors length optimization, this study involves the calculation of electric flux density and the charge induced. Now this section takes a closer look to the signals delivered by the sensors, their prediction and their application. There are four sensors that collect signals from the pipe. The first is designed to be close to the needle and long enough to collect the main injection. The other sensors are designed to sink the current due to charged powder when it discharges at the grounded pipe. †

The electric charge with respect to time can be evaluated, and the electric current which flows from the walls of the pipe to the ground can be predicted. According to the previous study, if the particles are flowing at constant velocity, it follows that.

$$x = V.t$$
$$dx = V.dt$$

Where V is the velocity of the powder. These are substituted below, hence

$$i(t) = dQ/dt$$
$$i(t) = V.dQ/dx$$

The second term of the last equation " dQ/dx ", can be deduced from the previous sections. It appears that the current is proportional to the velocity of the powder, and according to sensor and pulse length, $i(t)$ can be predicted.

In the next chapter the sensors that measure the charge induced are designed to capture the maximum charge, except the first sensor which is designed to measure the total charge injected. This can be obtained by using a sensor length of 31mm, which gives a total flux of 95% according to Fig 2.7

Chapter 3

SIGNAL PROCESSING

3.1 Introduction

A pulse charge is injected into the powder flowing in the pipe, this charge is then detected by sensors downstream, which act as current amplifiers and will detect charge deposited on the sensor or induced in it. The aim is to measure the total charge injected into the powder. To do this it is necessary to integrate the current which passes through the sensor, and then detect its highest peak.

Sensors are located along the pipe, and designed to read electric currents induced by charged powder inside the pipe. An electronic instrument based on analog circuitry, is built to measure the charge sensed at the sensors, however, the circuit accuracy depends on the way they are built. This chapter deals with the signal processing necessary to read different sensors simultaneously, and the circuit analysis of the important circuit elements, in order to reduce drift and noise in the instrument.

3.2 Signal processing

Four sensors collect signals from the walls of the pipe. The first one is designed to be close to the needle in order to sense the total charge injected. The three other sensors collect signals due to the flux induced by charged particles flowing in the pipe, and unaffected by the ions due to corona discharge, due to their distance from the point of injection.

The signal processing is based on the circuit diagram of Fig(3.1), which consists of four current to voltage converters. The second stage is to measure the charge induced.

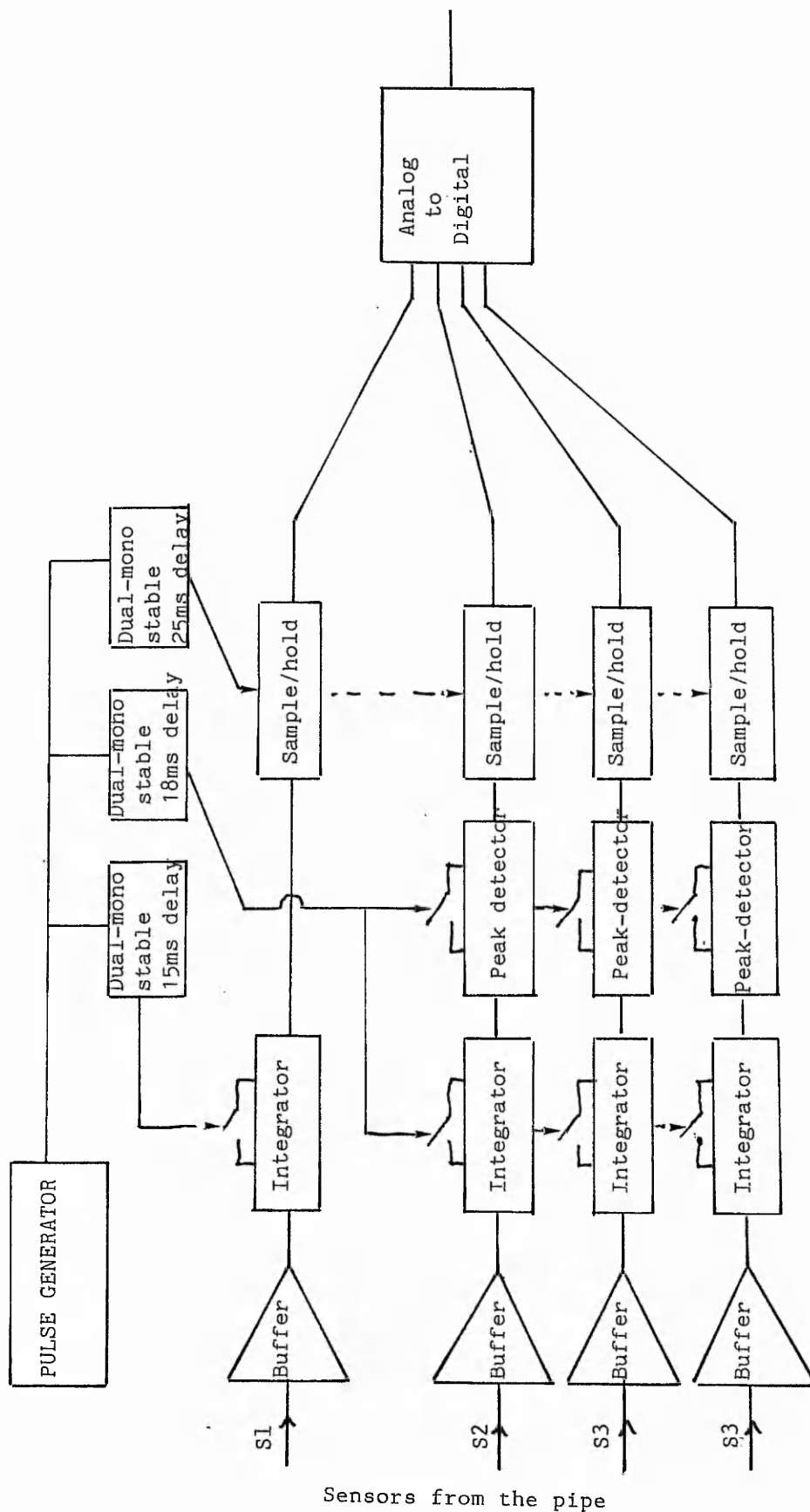


Fig 3.1 Circuit diagram of the analog circuitry

This consists of integrating the current. The integral of the signal coming from the first sensor equals to the total charge injected, but the integral of the other sensors give zero because the total flux induced by the particles is zero (section 2.5). Peak detectors are therefore needed to obtain the peak value of the charge. The third stage is the recording of the data using four sample and hold circuits.

Because of the time delay between signals when measuring the charge induced at each sensor, peak detectors and sample and holds are used to read all the sensors simultaneously. Timing necessary for this task is provided by dual monostables which are triggered by the pulse generator.

3.2.1 Peak detectors

A positive peak detector circuit follows the positive voltage and holds the maximum value attained in a capacitor. When this capacitor is discharged by a switch, the output goes to zero.

The circuit in Fig 3.2 consists of two LF351 JFET op-amps. The first one, A1, is a comparator which compares the input voltage with the last value stored in the capacitor. When the input voltage is higher than the value stored in the capacitor the diode D1 conducts, and the capacitor is charged to the new value. The second op-amp, A2, is a unity gain buffer. An analogue switch is used to discharge the capacitor and is operated by a dual monostable .

3.2.2 Sample and hold (S/H)

Four sample and hold integrated circuits AD 585 are used to sample the signals at $T = 20\text{ms}$. The control inputs of the S/H chip which allow the switching, on and off, between the sample and hold modes are delivered from the dual monostable in Fig 3.3.b.

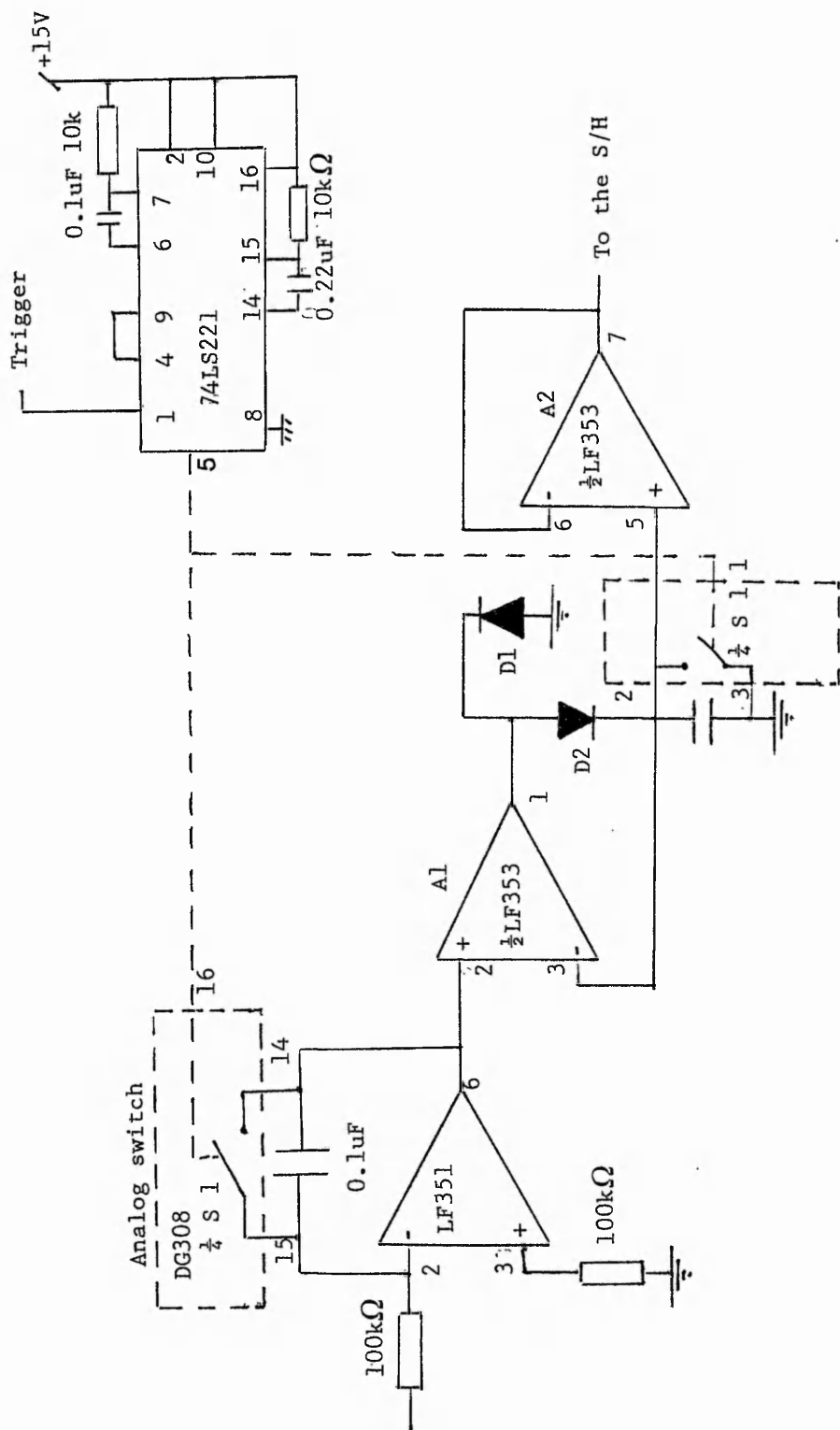


Fig 3.2

Integrator and positive peak-detector

The sample and hold circuit presents problems which involve the aquisition time and voltage droop in the hold mode . Large capacitors hold the signal for a long time with small droop, but the aquisition time, which is the charging time, is long. Small capacitors, in contrast, give a considerable droop, but a short time of aquisition . Aquisition time and droop are two parameters which cannot be fulfilled simultaneously.

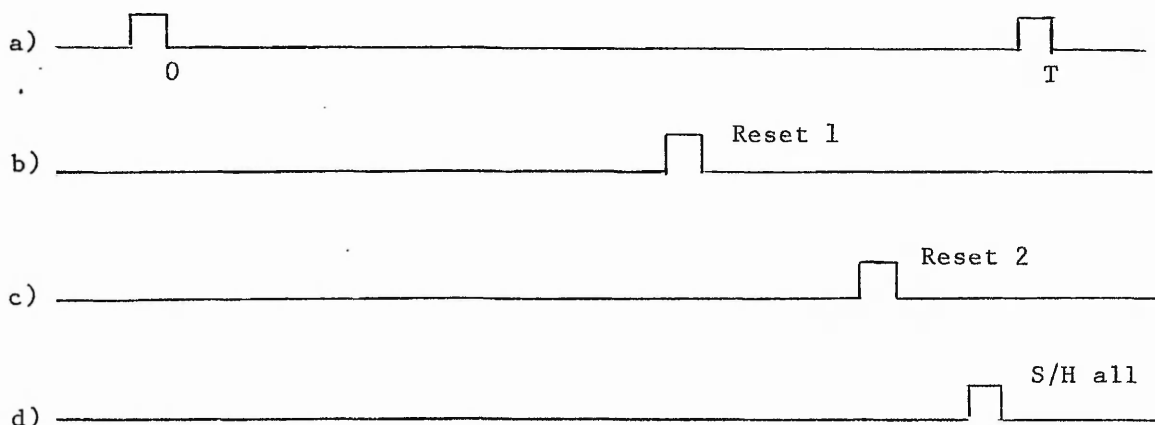


Fig 3.3.c

3.2.3 Timing diagram

As previously stated the peak detector and integrator need to be reset each cycle. The signal at one channel is shifted in time from the next one, therefore, dual monostables were chosen to generate the correct timing necessary to the reset all the integrators, and the S/H.

In Fig 3.3.c the signal " a " is the pulse which triggers the power supply and the dual monostables. Signal " b " is a delay of 15ms from " a " , which only resets the injection current integrator. The third pulse " c " is a delay of 18ms from " a " , resets all the other integrators and peak detectors. The fourth pulse " d " operates all the S/H all circuits at the same time.

3.3 Circuit analysis

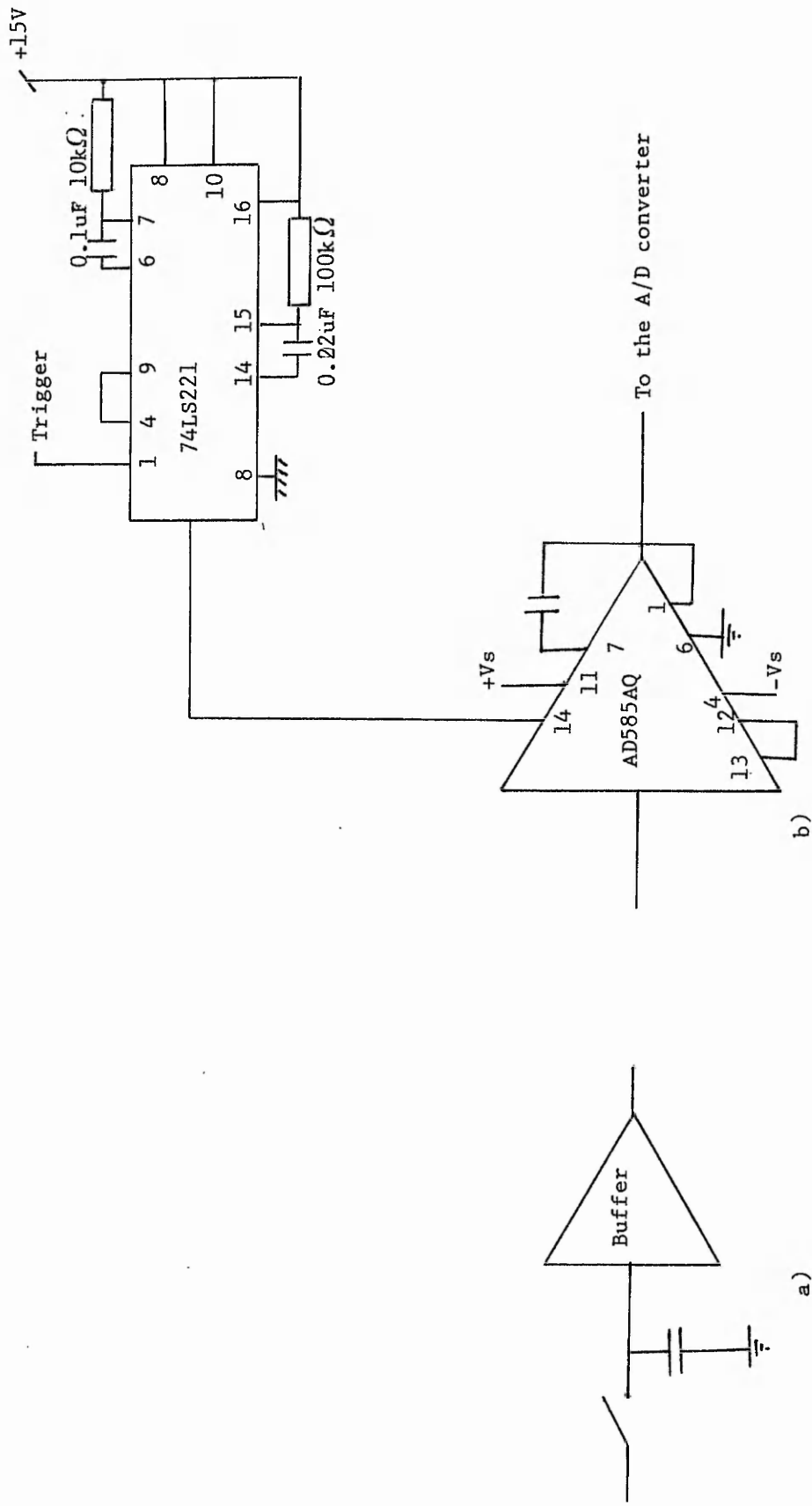


Fig 3.3

a) Ideal S/H, b) Pratical sample/hold

The aim of doing circuit analysis is to find the optimum circuit conditions, in order to minimize the errors in the circuit, such as drift and noise. The analysis is mainly based on the current to voltage converter and the integrator. Details of the analysis is in appendix B.

3.3.1 Current to voltage converter

A conversion from current to voltage must be done first because it is easier to deal with voltage rather than current, and operational amplifier circuits are then suitable for scaling the voltage.

The current to voltage conversion circuit analysis is based on the input impedance which is ideally equal zero, and the evaluation of the input offset current.

3.3.1.1 Current source

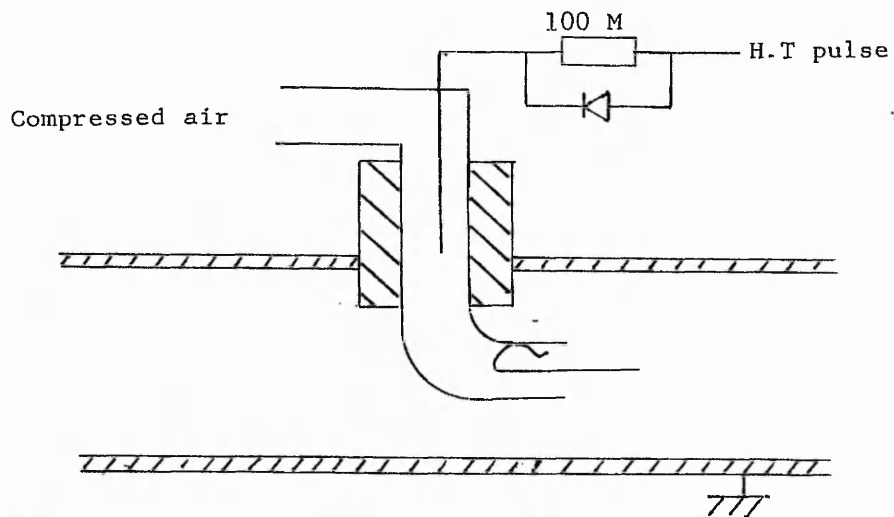
The sensor which delivers the current induced by the charges, in Fig 3.4.a, is a real current source, and Fig 3.4.c is its equivalent circuit. Where R_s is the internal resistor (resistance of the powder), and C_s is the internal capacitor, which is due to the cylindrical form of the pipe.

3.3.1.2 Input impedance

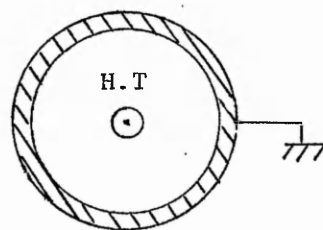
The ideal current to voltage converter circuit, provides a zero voltage drop, when using ideal op-amp, because the input impedance is an ideally equal to zero. Equation (3-1) gives the expression of the input impedance of a real current to voltage converter which is :

$$\frac{1}{Z_{inl}} = \frac{1}{Z_{inl}} + \frac{1+A_{ol}(\omega)}{R_2} (1 + jC_W R_2) \quad (3-1)$$

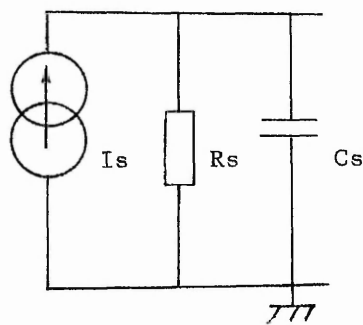
Where Z_{inl} is the open loop input impedance of a real



a)



b)



c)

Fig 3.4

- a) H.T pulse injection
- b) Cross-section
- c) Equivalent current source.

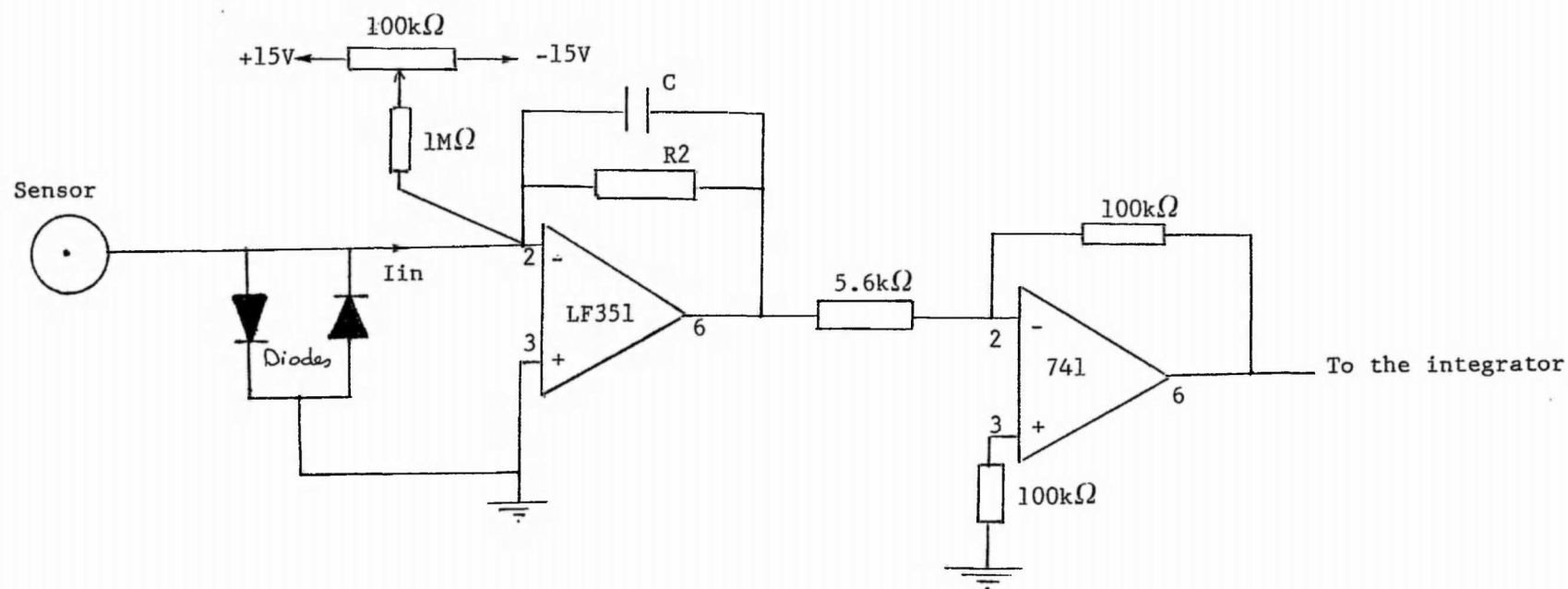


Fig 3.5

Current to voltage converter and amplifier

op-amp Z_{in1} is the closed loop input impedance, and A_{ol} is the open loop gain.

The analysis shows that Z_{in1} is close to zero when using a JFET op-amp, because of its high open loop input impedance, which is $Z_{in0} = 10^{12} \Omega$

For a DC and low frequency signal, the open loop gain, $A_{ol} = 110$ dB. If $R_2 = 10k\Omega$ and $C_f = 0.01\mu F$, it makes $Z_{in1} = 0.03 \Omega$. Suppose the current to be measured is $I_{max} = 10$ μA then the voltage drop is $I_{max} Z_{in1} = 0.33$ μV .

3.3.1.3 Input offset current

Ideally the current that flows in the feedback branch, is equal to the input current, however, an error is introduced. Appendix B shows that the input error current is equal to

$$I_{os} = + \frac{V_{io}}{R_s // R_2} + I_{io} \quad (3-2)$$

Where R_s : is the internal current source resistor

V_{io} : is the offset voltage

I_{io} : input offset current.

The error is reduced by a large value of R_2 as long as the input impedance remains small.

3.3.2 Integrators

Although the current to voltage converter is well designed to measure the current, reading the charge is much easier than the current, because the current measurement ideally needs two peak detectors one for the positive peak and one for the negative peak, whereas the charge measurement only needs one. In order to get the charge carried by the powder, the output from the current to voltage converters is then integrated. Using an integrator circuit, such as the one presented in Fig 3.2, would solve the problem. However, problems occurs when using the integrator circuit. Here are details of these and some technical solutions.

3.3.2.1 Offset and drift errors

The greatest error of an integrator comes from the offset voltage and drift. Equation (3-4), given in appendix B, presents an expression of the output voltage of a real integrator, taking into consideration the input offset voltage, V_{io} , and the input bias current, I_b .

$$e_o = - \int_0^T \frac{e_{in}}{RC} dt \pm \int_0^T \frac{V_{io}}{RC} dt + \int_0^T \frac{I_b}{C} dt \pm V_{io} \quad (3-4)$$

Where e_{in} is the input voltage, e_o output voltage and T the period of integration. The error due to the input bias current I_b , of the amplifier, can be reduced by using an equal resistor to that of the integration, between the earth and the non-inverting input, whereas V_{io} can be reduced by a long period of integration 'RC'.

A real op-amp could never give an ideal integration, because of its finite bandwidth, and its open loop gain. Finite open loop gain causes errors at low frequency, and finite bandwidth causes errors at high frequency.

3.3.2.2 Practical consideration

Good integrators use low input current FET op-amps such as the LF351 (input bias current of 50pA) or BIFET op-amp such as the TL071 (30pA). They allow the input bias current contribution to the integrator drift to be negligible without the use of an excessively large capacitor values.

The examination of equation (3-4) suggests that large values for the capacitor might reduce the drift, but the resistor needs to be small to keep the same RC value. Because R is the input impedance of the circuit, a lower limit exists on R because of a current limitation.

Polystyrene and teflon are usually the best capacitor choices for long term integration accuracy. Capacitor leakage presents an additional source of integrator drift. A capacitor whose dielectric leakage current is less than the amplifier bias current must be used. The choice of the amplifier is also governed by the length of time of integration and desired accuracy. In general op-amps used for different lengths of time are :

- Chopper-stabilized amplifier for long time.
- FET amplifier for medium length of time.
- BIFET amplifier for a short time.

For the present circuit the amplifier used is FET, and $R = 100k\Omega$, $C = 0.1 \mu F$ which makes $RC = 0.01s$, and an input current of $10\mu A$ which compared with input current error is extremely small.

3.5 Noise analysis

Measurement of DC voltages cause some problems, especially if small voltages are involved, thus a practical limitation for every type of instrument exists. Input stages of DC voltages can be improved by examination of drift, noise and sensitivity. Drift is the instability of the instrument in terms of temperature variation. Sensitivity is the minimum amplitude of signal that the equipment is capable of resolving. Noise is a random, unpredictable voltage wave form that contaminates the signal.

3.5.1 Basic properties of noise

The noise falls into two main categories, which are white noise and flicker noise ($1/f$). The density of a white noise is independent of the frequency f , whereas the flicker noise density varies on $1/f$. Here are examples of white noise which are thermal noise and shot noise.

(a) Thermal noise is generated by random agitation of electrons, which manifests by an increase in temperature.

Resistor noise is an example of the thermal noise, where the mean square of the noise voltage in a narrow frequency band width is equal to:

$$\overline{V_n^2} = 4kTR \, df \quad (3.1)$$

Where T is the temperature in degrees Kelvin (K), and k is Boltzmann's constant.

(b) Shot noise (Schottky noise) is due to random emission of electrons from the cathode in diodes. Each emission arriving at the anode carries a discrete electronic charge, q, which gives rise to a current pulse during the transit time. The mean square value of the current noise is:

$$\overline{I_n^2} = 2qI \, df \quad (3.2)$$

Where I is an external current flowing through the diode.

Flicker noise on the other hand, is the most critical noise source, generated by thin metallic or semiconductor layers, by carbon resistors and solid state devices. The power spectral density of noise is:

$$s^2(f) = K \frac{1}{f} \quad (3.3)$$

Where K is the value of $s(f)$ at 1 Hz.

The noise generated in op-amps is a combination of white noise and (1/f) noise. The total mean square input of both current and voltage noise, V_{nt} and I_{nt} of an op-amp are

$$\overline{V_{nt}^2} = \left[v_n^2 \left(1 + f_{ce} \frac{1}{f} \right) \right] df \quad (3.4)$$

$$\overline{I_{nt}^2} = \left[i_n^2 \left(1 + f_{ci} \frac{1}{f} \right) \right] df \quad (3.5)$$

Where i_n , v_n are respectively noise spectral densities of the current and voltage of the op-amp in Fig 3.6.a, and f_{ce} , f_{ci}

are corner frequencies relative to the current and voltage source of noise.

3.5.2 Signal to noise ratio

Signal to noise ratio, $SNR = S/N$, is defined as the ratio of signal power to noise power. The ratio is minimum when the signal is contaminated by a high level of noise.

It is proposed to measure the noise produced by the instrument, then optimize it by minimizing the sources of noise. The analysis here is based upon the current to voltage converter as the the first stage where the noise may be reduced. The signal to noise ratio calculation consists of evaluating the total equivalent output noise voltage. The equivalent circuit of the current to voltage converter source of noise in Fig 3.6.b can be used to sum the total input current noise density, i_{nt} , which is.

$$i_{nt}^2 = 4kTR(f)/(Z//R_s) + i_n^2 + v_n^2/(Z//R_s) \quad (3.6)$$

Where $R(f) = R / [1 + (2\pi RCf)^2]$, is the resistive component of the impedance, Z . The current source resistor R_s is due to charged particles at high voltage and the current flowing to the ground is about 0.1 uA, hence the resistor R_s is ideally infinit, which makes $(Z//R_s) = Z$.

A noise evaluation requires a knowledge of the spectral distribution of the input noise source $s_n(in)$. These are multiplied by the frequency dependent square magnitude of the transfer function and appear at the output as output spectral density $s_n(out)$. This is illustrated by equation (3.6).

$$s_n(out) = s_n(in) |H(f)|^2 \quad (3.7)$$

Where $H(f)$, is the transfer function, which in the case of the current to voltage converter is the feedback impedance.

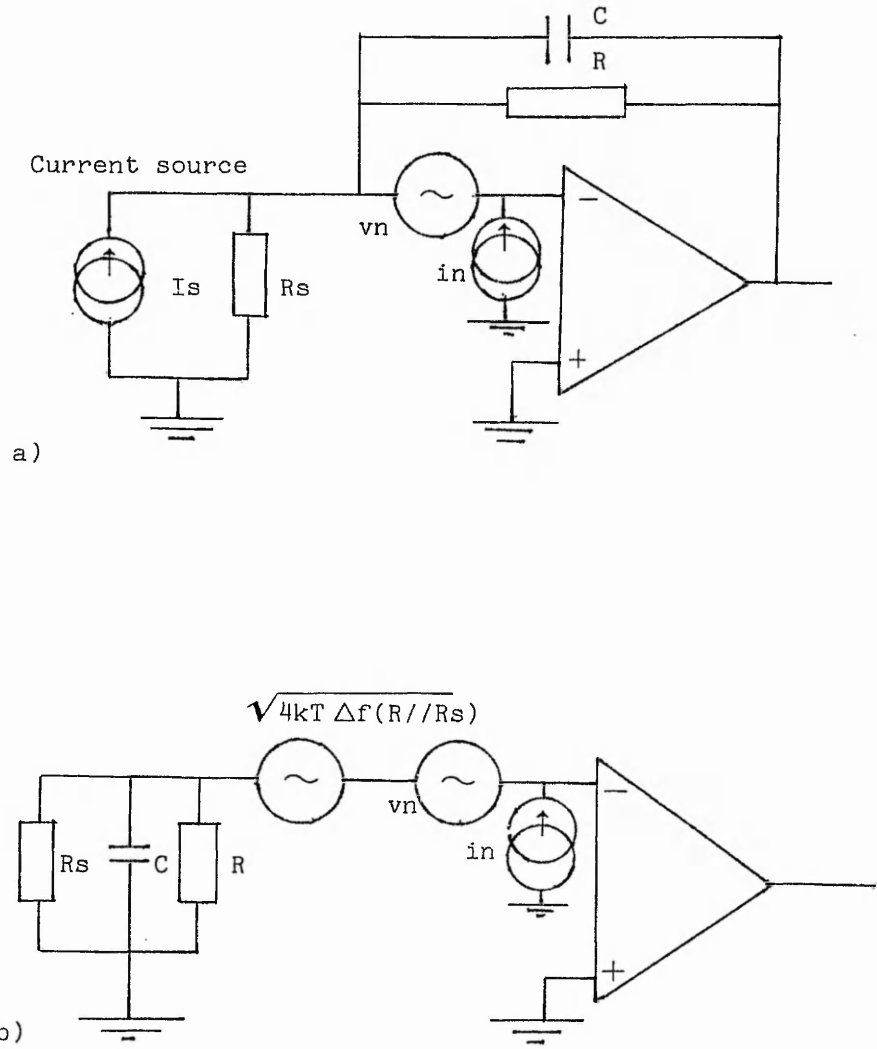


Fig 3.6

Current to voltage converter source of noise

$$|H(f)|^2 = Z^2 = \frac{R^2}{1 + (2RC\pi f)^2}$$

The input noise spectral density is the total current, i_{nt} , and The output noise spectral density is the total voltage noise, v_{nt} , which is.

$$v_{nt}^2 = i_{nt}^2 \cdot Z^2 = 4kTR(f) + i_{n^2} Z^2 + v_n^2 \quad (3.8)$$

The last term of (3.8) is multiplied by the noise frequency band width, Δf , whereas the first two terms are integrated

upon the entire frequency spectrum. The mean square output noise voltage, taking into account only the white noise is:

$$V_{nt}^2 = \int_0^{\infty} (4kTR + i_n^2 R^2) \frac{1}{1 + (2\pi RCf)^2} df + v_n^2 \Delta f \quad (3.9)$$

The integral of the above expression is

$$V_{nt}^2 = (4kTR + i_n^2 R^2) \frac{1}{4RC} + v_n^2 \Delta f \quad (3.10)$$

The first term of (3.9) may be calculated other ways, by multiplying the resistor, R , by the noise band width, Δf . This is because the power generated by the resistor R is transferred to the resistive impedance.

$$\frac{kT}{C} = 4kTR \Delta f \quad (3.11)$$

$$\Delta f = \frac{1}{4RC}$$

When replacing the value of, Δf , at the last term of (3.10) the final expression is:

$$V_{nt}^2 = \frac{kT}{C} + \frac{i_n^2 R}{4C} + \frac{v_n^2}{4RC} \quad (3.12)$$

Finally the numerical value of (3.13) is obtained by the choice of $RC = 0.001s$, and the LF351 op-amp source of noise $i_n = 0.01pA/\sqrt{Hz}$, $v_n = 16nV/\sqrt{Hz}$, hence :

$$V_{nt} = 0.473 \text{ uV rms}$$

The output signal power, S_o , is obtained using (3.7), where the input current signal is about, $I_{in} = 0.1 \text{ uA}$, and the transfer function is $R = 10 \text{ k}\Omega$, thus $S_o = 1mV$. Hence the the signal to noise ratio, $SNR = S_o^2 / V_{nt}^2$, is maximum enough for the present application.

Chapter 4

INTERFACE WITH A MICROCOMPUTER

4.1 Introduction

The previous chapter dealt with the analysis of the analog circuitry of the instrument that measures the charge induced. The instrument is applied to the mass flow rate measurement in order to study the correlation between the data recorded and the measured mass flow rate. However, this process can not be done manually as the large volume of data needed will take too long to collect. In this chapter the electronic instrument is interfaced to the BBC microcomputer. The interfacing has two parts, the software, and the hardware. The hardware contains an analog to digital converter, and a buffer which is connected to the user port. The software is based on the main program that records the data, and the processing is based on programs that evaluate the correlation.

The BBC microcomputer comprises a 6502 central processing unit (CPU), with 64K memory, 32K of which is ROM containing the operating system, and 32K of user accessible RAM. For full analysis and system simulation, the BBC microcomputer can not be used due to its small memory capacity and slow processing speed. For this operation a mainframe or minicomputer is needed. The task of the BBC however, was to gather the data and perform simple error bar and standard deviation analysis. The BBC could actually be used to control the flow system and this is discussed in chapter 6.

4.2 Hardware

The circuit diagram of the hardware, Fig 4.1, consists of the analog electronics, described in chapter 3, which measures the charge collected by the sensors. These signals

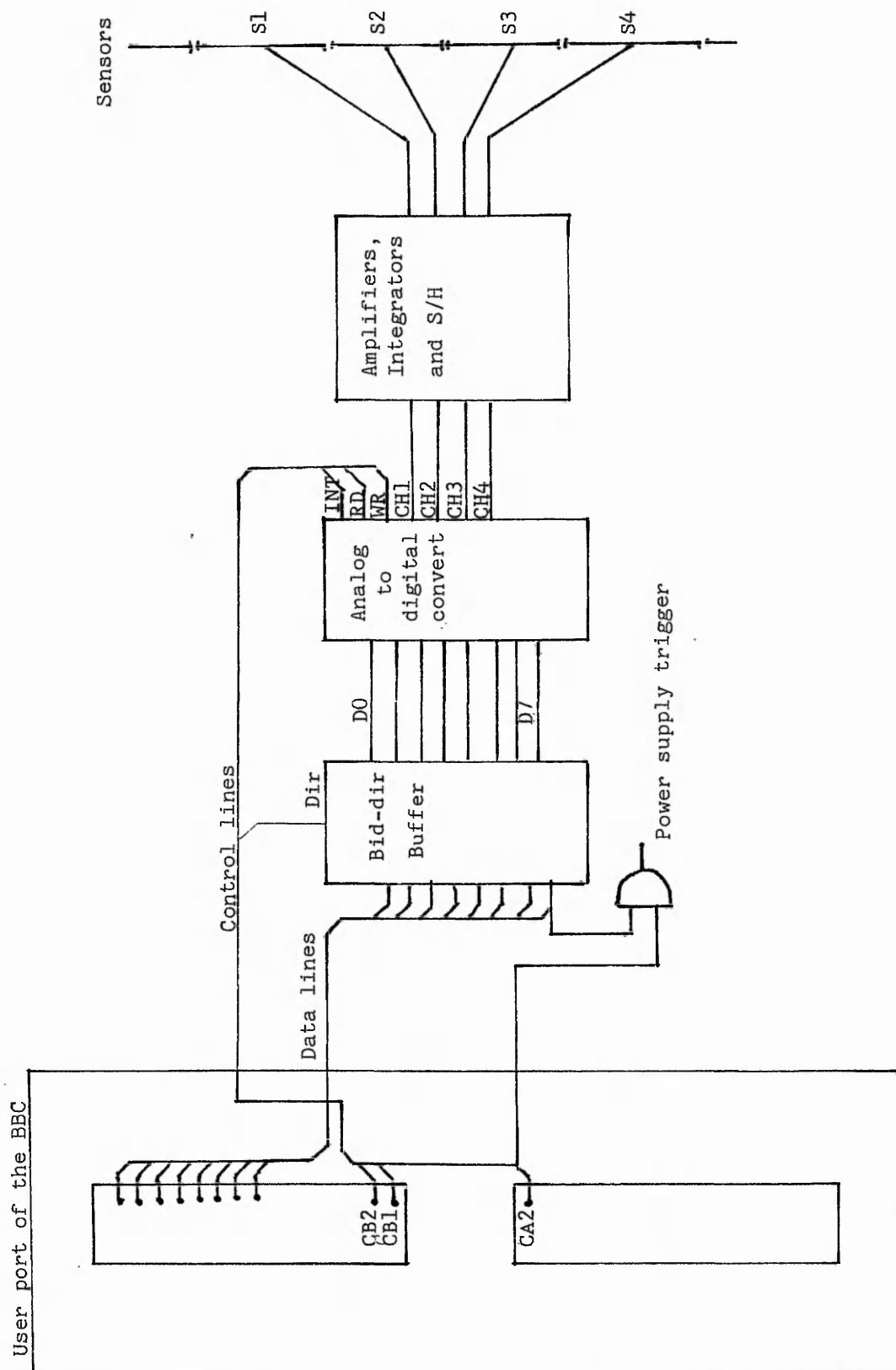


Fig 4.1

Block diagram of the interface, user port and ADC

are processed by a multiplexed analogue to digital converter, which replaces the ADC of the BBC.

4.2.1 User port of the BBC

The input/output ports of the BBC use a powerful and flexible interface circuit, the versatile interface adaptor (VIA) 6522 Fig 4.2.a. The VIA is a combination of peripheral interface adaptor PIA and asynchronous communications interface adaptor ACIA. The VIA contains two identical 8-bit registers which can be programmed either as input or output, plus a number of control lines such as CB1, CB2, CA1, CA2 (used for handshaking). There are two 16 bit programmable timer/counters, and a serial to parallel / parallel to serial shift register.

4.2.2 Analog to digital converter

The user port of the BBC used as input and output, contains eight data lines and two control lines CB1 and CB2, only the data lines are buffered by a bidirectional buffer 74LS245. The control line CA2 of the printer was used to set the direction of the buffer. The A to D converter used was an ADC00844 Fig 4.2.b, a CMOS 8-bit successive approximation converter with versatile analog input multiplexers. The 4-channel multiplexers can be software configured.

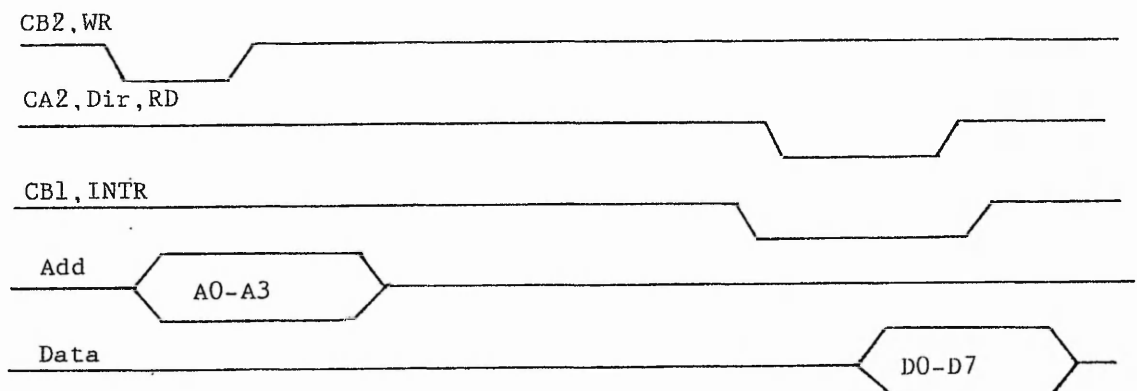


Fig 4.2.c
Timing diagram of the A/D converter

The timing diagram above, Fig 4.2.c, shows that the ADC needs only three control lines from the user port to read an analog input. The control line CB2 starts conversion, CB1 is used as the end of conversion signal or interrupt, and CA2 is used to reset the interrupt and set the direction of the buffer.

4.3 Software

The software, as previously stated, is based. Firstly on the main program that triggers the pneumatic system and records the data. Secondly, data processing that evaluates the error and correlation.

4.3.1 Main program

The flowchart of Fig 4-3 describes the software written in BASIC. The program starts by triggering the power supply, then reading the voltage held by the S/H, using the A/D of the BBC. The same operation is repeated a hundred times, and the average is recorded before a new value of the flow, is set by adjusting the valves manually. After running the program for several values of flow rate, the program starts plotting the graph of the ratio $Q2/Q1$ against the mass flow rate, or saves the results in a data file known in section 4.4.3 as the first type of graph.

The second idea was to generate a program which would record the ratio $Q2/Q1$, N times for each value of the flow, each time taking an average of 100 readings, then finding the error bar or the standard deviation. The A/D converter of the BBC, is too slow to read $100 \times N$ (where $N = 100$) in the required time, therefore, the A/D was replaced by an external one. This needed a program written in 6502 assembly language to control the A/D.

The assembly language software consists of four routines. The first routine clears three pages of memory. The second

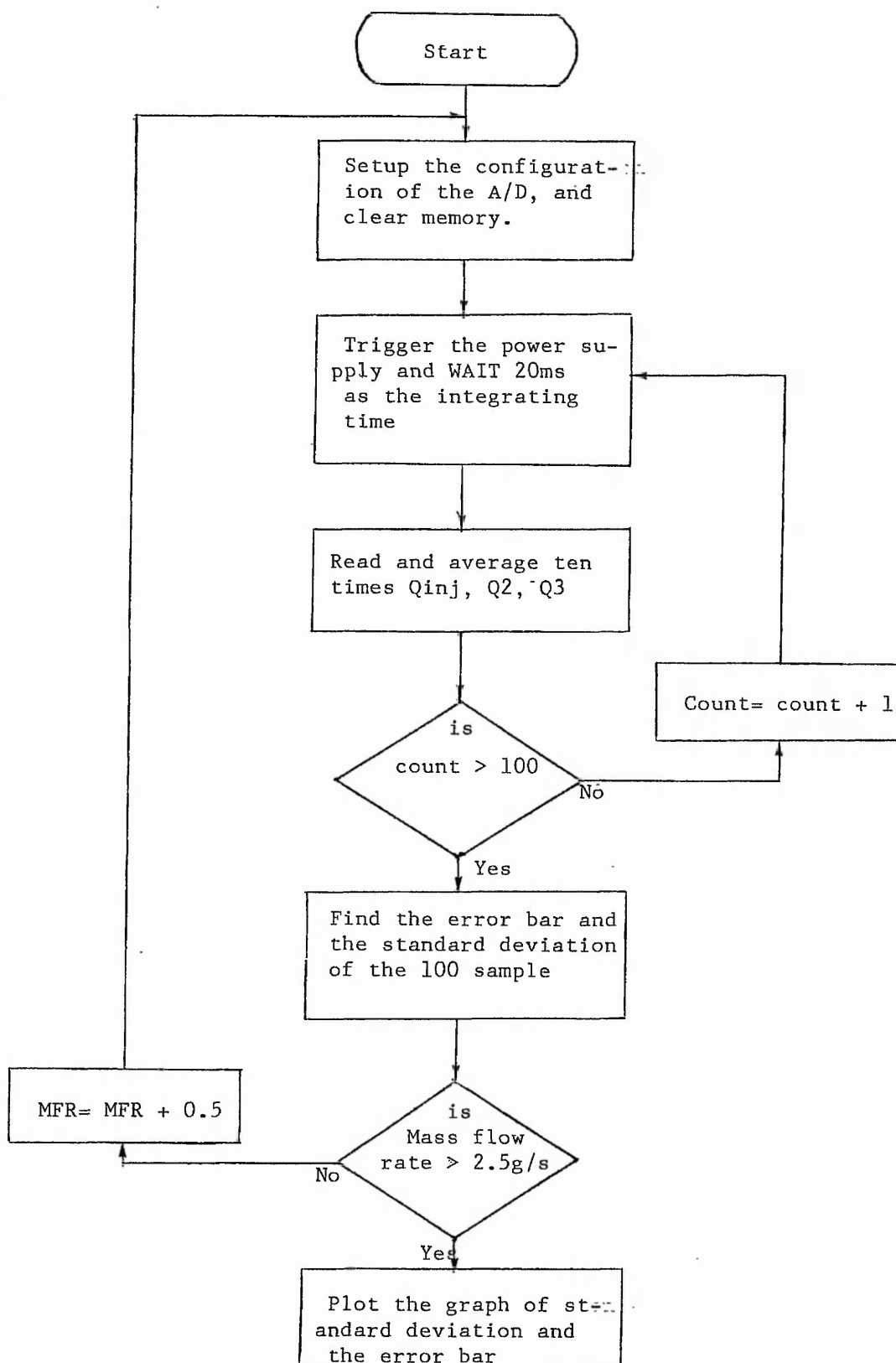


Fig 4.3

Flow chart of the data record and analysis

routine triggers the power supply and waits 10ms, and the third routine reads the A to D converter. Ten such readings are then averaged to produce the final result.

4.3.2 Data processing routine

The data processing software contains the error bar and the standard deviation calculation. The flow chart of Fig 4.3 shows the data processing procedure, which consists of opening four data files, finding the error bar and the standard deviations for each file, then plotting all the standard deviation on one graph.

The aim of this analysis was to study the fluctuation of the flow. The ratio $Q2/Q1$ is one of many parameters which predict the flow, and this appears to yield a stable result.

Chapter 5

EXPERIMENT AND RESULTS

5.1 Introduction

Interfacing with the microcomputer makes it easy to operate the experiment, especially the data recording. This chapter contains an experimental procedure of the mass flow rate measurement, and data analysis. It also contains a study of the relationship between the actual mass flow rate and the measurement given by the instrument.

Experimental procedure explains how the flow can be measured using the pneumatic system and analog electronics. Comment on the results recorded by the experiment are given. Data analysis consists of evaluating the error or spread of the data recorded by means of standard deviation, and the mean value.

Initially the type of powder used was a white epoxy/polyester, which is the one used by C.Willis and B.C.O'Neill [1]. Later the powder was mixed with a black one of similar type. The latter seemed to have heavy particles, in contrast with the former which has finely divided dust.

5.2 Experimental procedure

When using the pulse charge injection technique, the mass flow rate measurement is obtained using a set of electronic and pneumatic instruments. The three main parts which contribute to the experiment are, the high voltage power supply, the electronic equipment, and the pneumatic system. Here is a description of each part of the experiment.

5.2.1 Pneumatic system

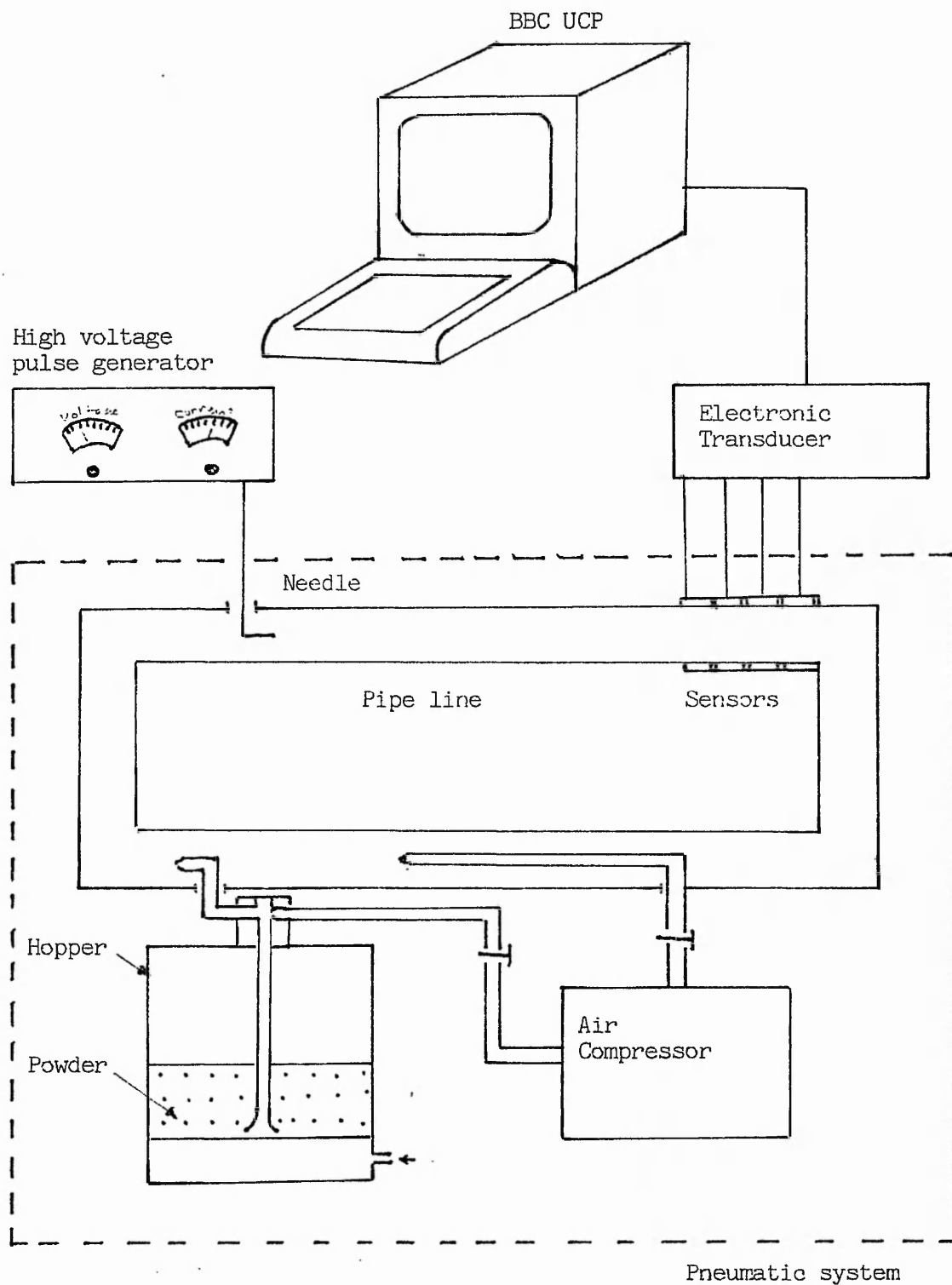


Fig 5.1

Experimental procedure, schematic diagram

The pneumatic system consists of a compressor, which delivers the air to a hopper which contains the powder, cylindrical pipes in which the powder flows and the sensors are located. Valves control the mass flow rate by adjusting the flow of the primary and secondary pipes which feed the hopper.

First the hopper is fed with a suitable sort of powder. Two types of powder have been used so far, both are polyester/epoxy, the first white and the second black. The experiment shows that the second type induces less current than the first one, later the second type of powder started inducing higher currents. Two parameters in the powder may affect the flow, these are particle size and resistivity. The case for particle size is that after a long period of operation, the powder is pulverized (reduced in size), and the currents have been seen to increase with prolonged use of the powder. In fact that is one of many parameters which cause data fluctuations.

Secondly the compressor is switched on at a pressure level of (100 bar). The air delivered is assumed to be free of hydrocarbon gases, although it does contain a small proportion, which makes the powder wet. Finally the flow rate is set to the desired value by means of primary and secondary air valves .

5.2.2 High voltage power supply

Once the flow rate is set at a specific value, the high voltage pulse generator is triggered by a pulse generator of variable frequency and pulse width. The power supply is a high voltage pulse generator, which can deliver a maximum voltage of 15 kV, and a maximum current of 100 uA. Later the power supply was triggered by the BBC microcomputer for the analysis stage.

5.2.3 Analog circuitry

When using the electronic instrument designed to measure the charge induced at the sensors, it is important to see the currents induced at the sensors on the oscilloscope, as they vary with respect to time. The graphs in Fig 5.2 show that the currents induced are shifted in time, according to their position in the pipe, in fact this is due to the velocity of the particles which is defined as

$$v_1 = \frac{S}{\Delta t}$$

Where Δt is the time delay, between two successive peaks, and S is the sensor length .

Channel 1 the first sensor, detects the main injection is called the current injection, and Fig 5.2 shows that this is the sum of two current given below as

$$I_1 = I_{inj} + I_{cap}$$

Where I_{inj} is the main injection current, and I_{cap} is the capacitance current due to the cylindrical capacity of the pipe. The dielectric will vary with the concentration of the flow, I_{cap} , is smaller at high mass flow rates.

The final stage of the analog circuitry detects the maximum value of charge for each channel and holds it by means of a sample and hold circuit. The output of this circuit was connected to a high impedance digital voltmeter at the beginning of the experiment, in order to record data manually. This proved to be unsatisfactory, so the idea of interfacing the analog circuitry with a microcomputer came about.

5.3 Data processing

At the beginning data was recorded manually. This proved to be difficult to process the, since the experiment may be repeated several times. What follows is a description of the main elements involved in the data analysis, which enable

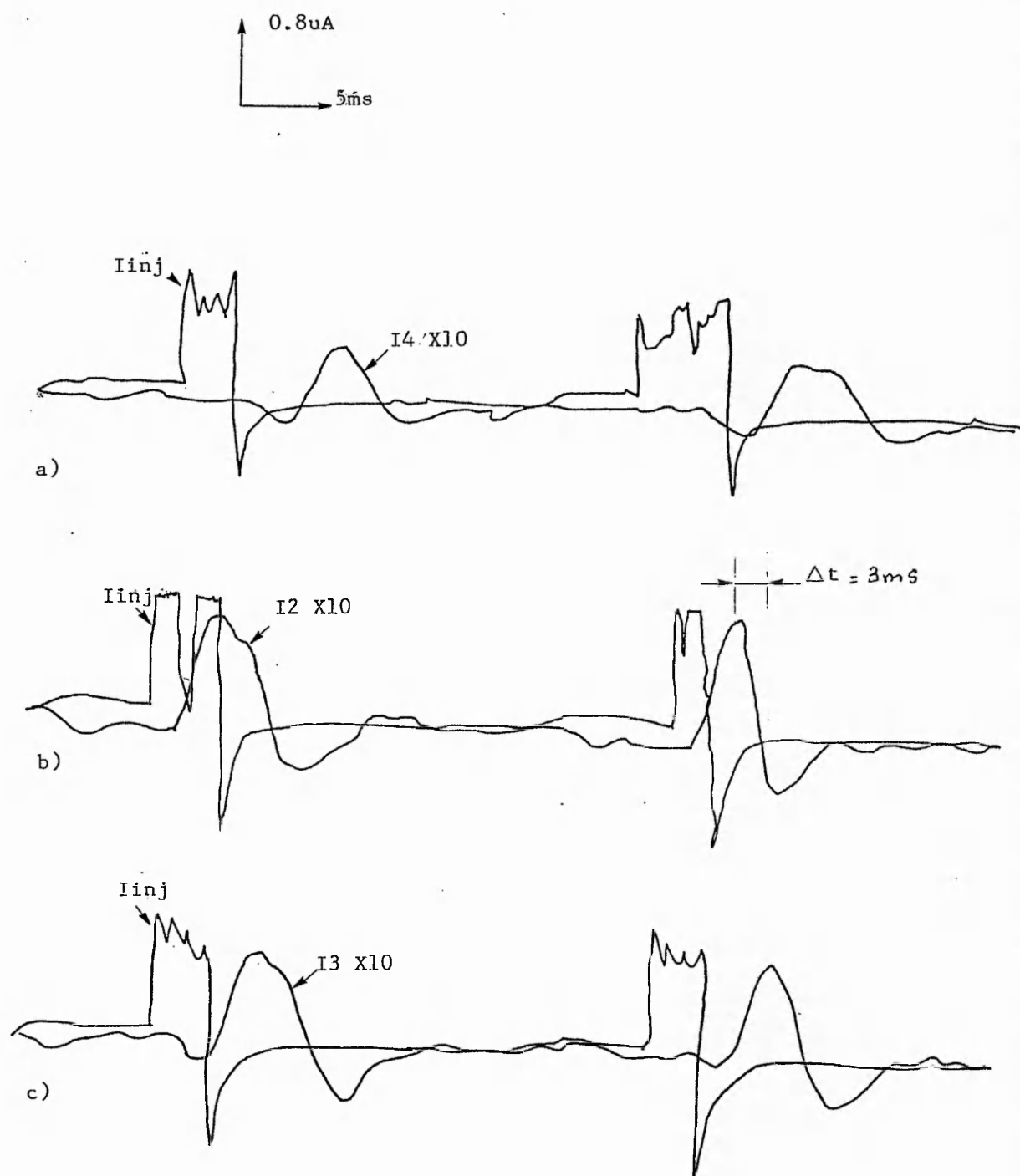


Fig 5.2

Current induced at the walls, time delay between sensors

mass flow rate prediction.

5.3.1 Mean absolute deviation (MAD)

The mean absolute deviation is defined as the average distance from data to the mean value. This can be written as

$$MAD(x) = \text{sum } |x_i - x| / n$$

Where x is the mean value of the data, and n is the number of samples. The mean value and error bar analysis were first carried out on the data, but later it appeared that this does not give an accurate description of the data spread.

5.3.2 Standard deviation

Its only the standard deviation that can show how stable the reading is, because it depends on the density of the spread. The error bar in contrast, can show only how wide the spread is. Standard deviation is defined as

$$s^2 = \frac{\sum_{i=1}^n \{\bar{Q} - Q_i\}^2}{n + 1}$$

Where Q is the mean value or average. Software written in BASIC was generated for both the error bar and the standard deviation calculations, in appendix D.

5.4 Results and discussion

The results and discussion are based on the measurement of charge deposition, given by the electronic instrument, and the ratio of charges as prediction parameters.

5.4.1 Comment on Q1, Q2, Q3.

The data recorded shows that the value of Q_1 (the main

injection) is higher at low flow rates than at high flow rates, whereas the charges Q_2, Q_3, Q_4, \dots are smaller at low flow and higher at high flow. Further down-stream these became almost equal.

The difference $D_i = (Q_i - Q_{i+1})$ gives the loss of charge between one channel to the other, due to particles which stick on the walls, and other parameters. At high flow rates the difference, D_i , gets smaller.

5.4.2 Discussion on the ratio Q_{i+1}/Q_i

As previously mentioned , section 5.4.1, at a very high flow rates Q_{i+1}/Q_i is nearly unity, while for lower rates there is a fairly linear relationship. It appears that only the ratio Q_2/Q_1 is appropriate to analyse, the ratios Q_3/Q_2 and Q_4/Q_3 being almost unity. Three types of graph have been recorded in order to analyse the ratio Q_2/Q_1 , starting with the averages to the error bar, and finally the standard deviation.

The first graph in Fig 5-3, shows the ratio Q_2/Q_1 against mass flow rate, each point represents an average of 100 samples. The maximum flow rate used is 1.2 g/s.

The second graph in Figs 5-4 and 5-5 shows the error bar of the ratio Q_2/Q_1 at different mass flow rates. These shows that the samples are almost linear within an error bar + 10 %, whereas at high flow rates they are not. This graph was produced for the evaluation of the spread of the recorded data and does not give total information of about the flow.

The third graph in Figs 5-6 and 5-7 represent the standard deviation of the ratio against the mass flow rate. This graph is used in study of the stability of the ratio of Q_2/Q_{inj} . The maximum flow rate here is at 2.8 g/s. The graph shows that the standard deviation, s , is within + 5% of the ratio Q_2/Q_{inj} .

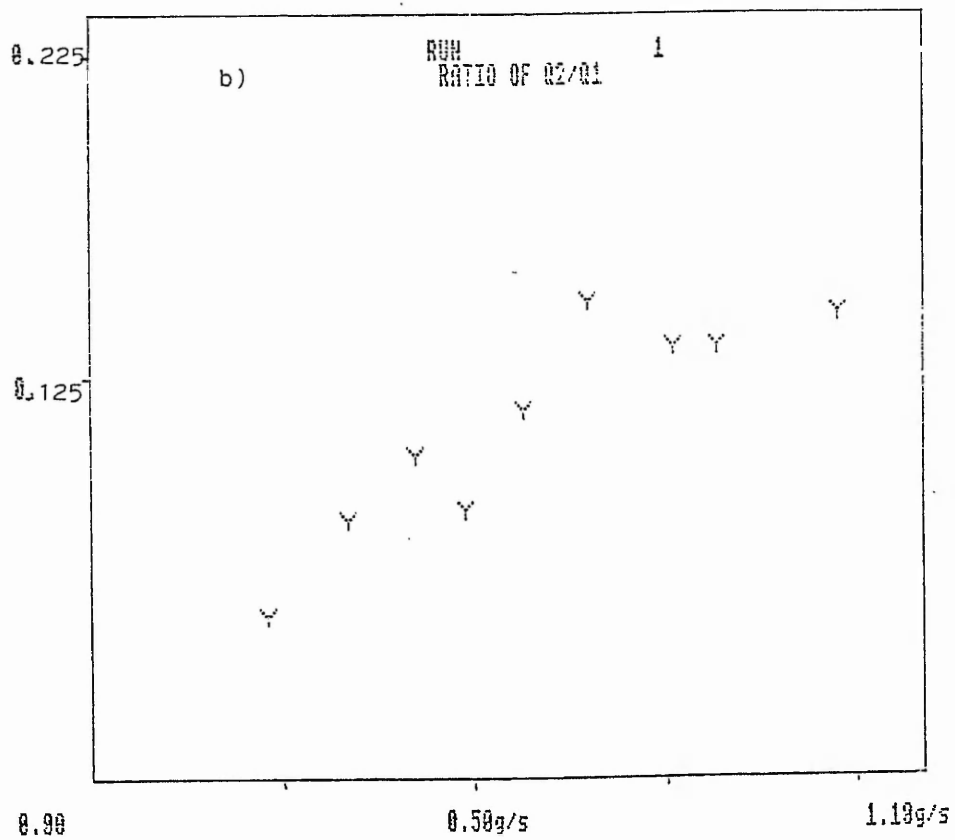
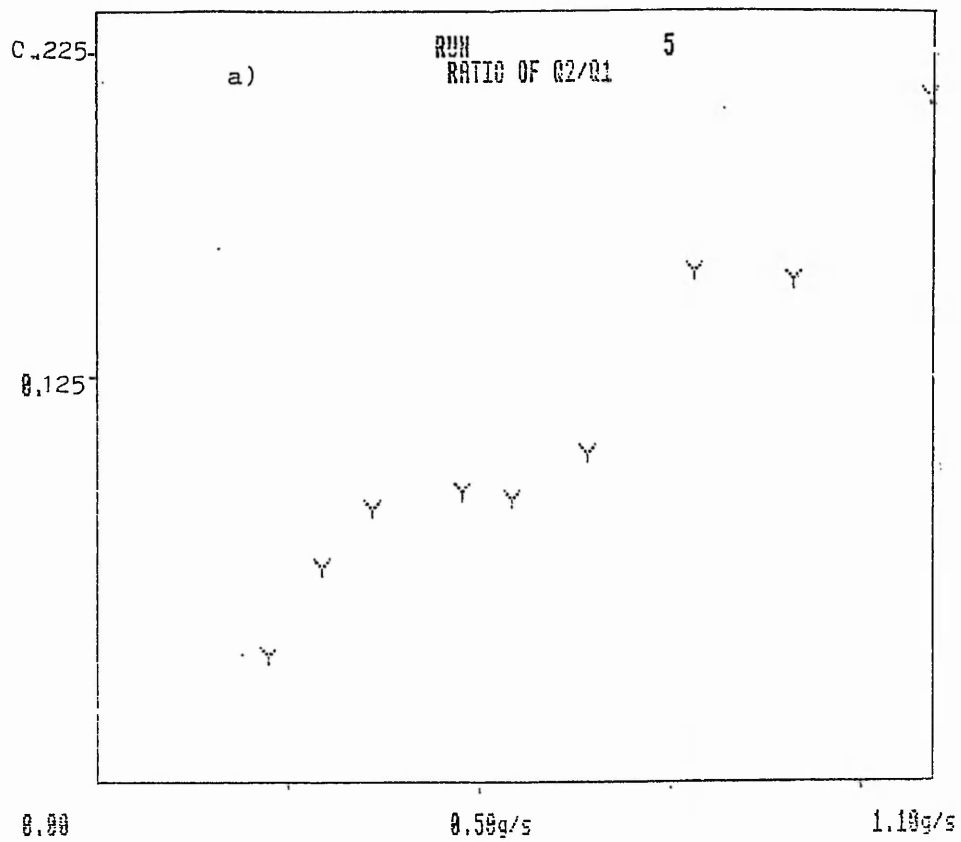


Fig 5.3

Data analysis: ratio Q2/Q1 with respect to M.F.R

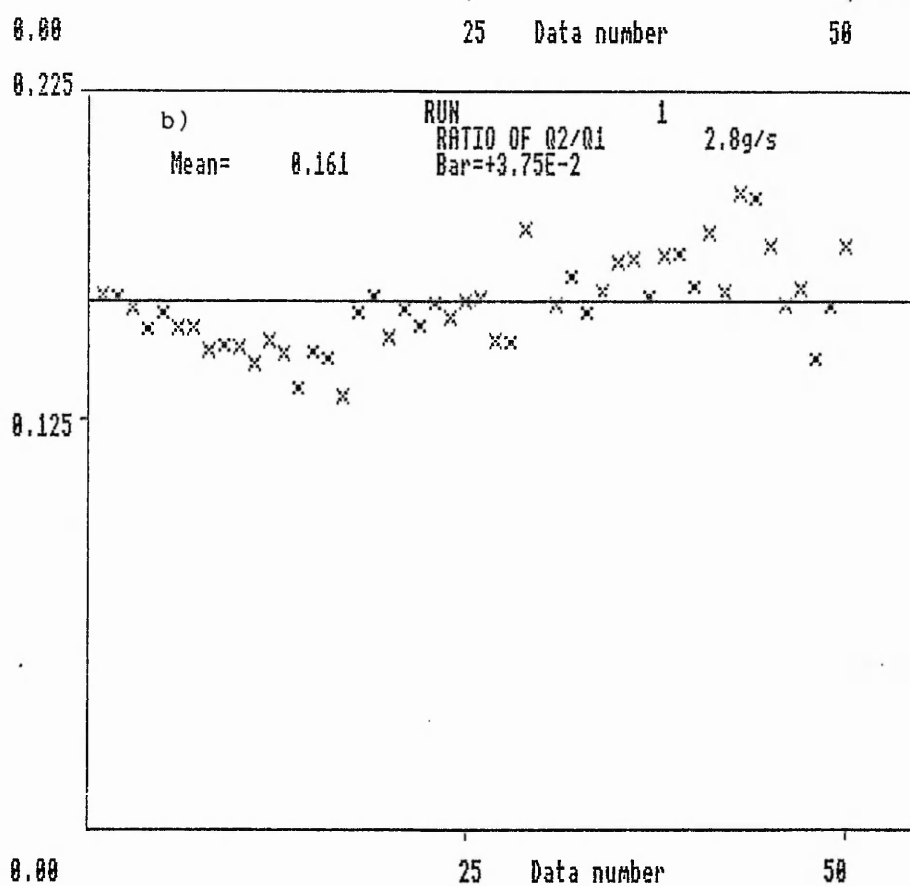
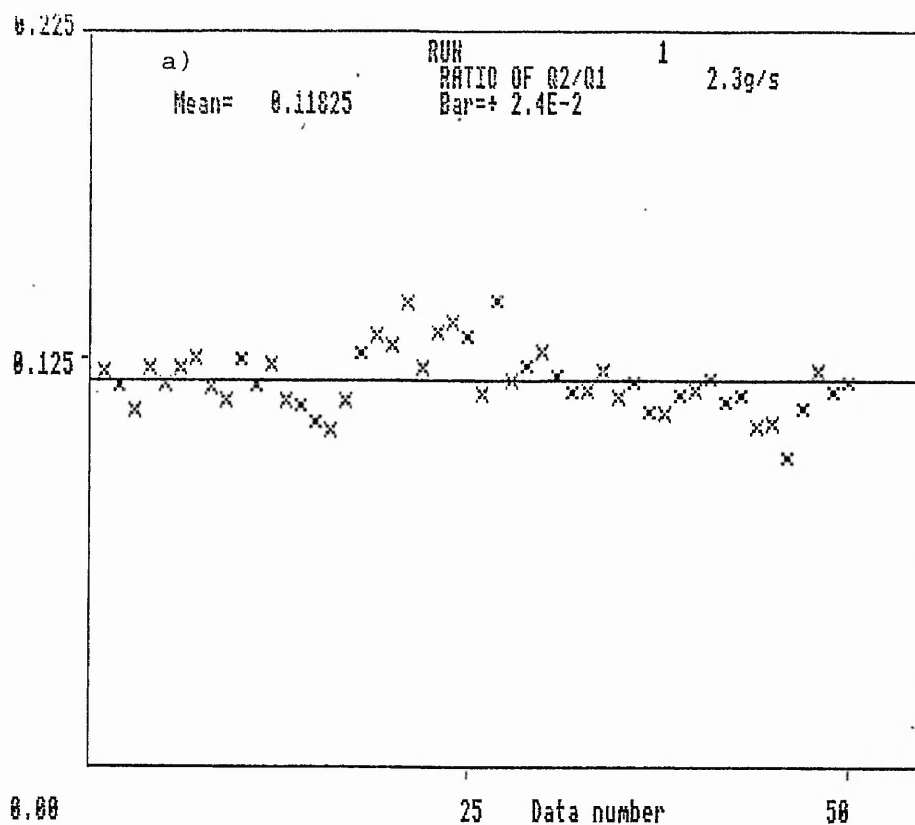


Fig 5.4

Data processing, error bar and mean value of Q2/Q1

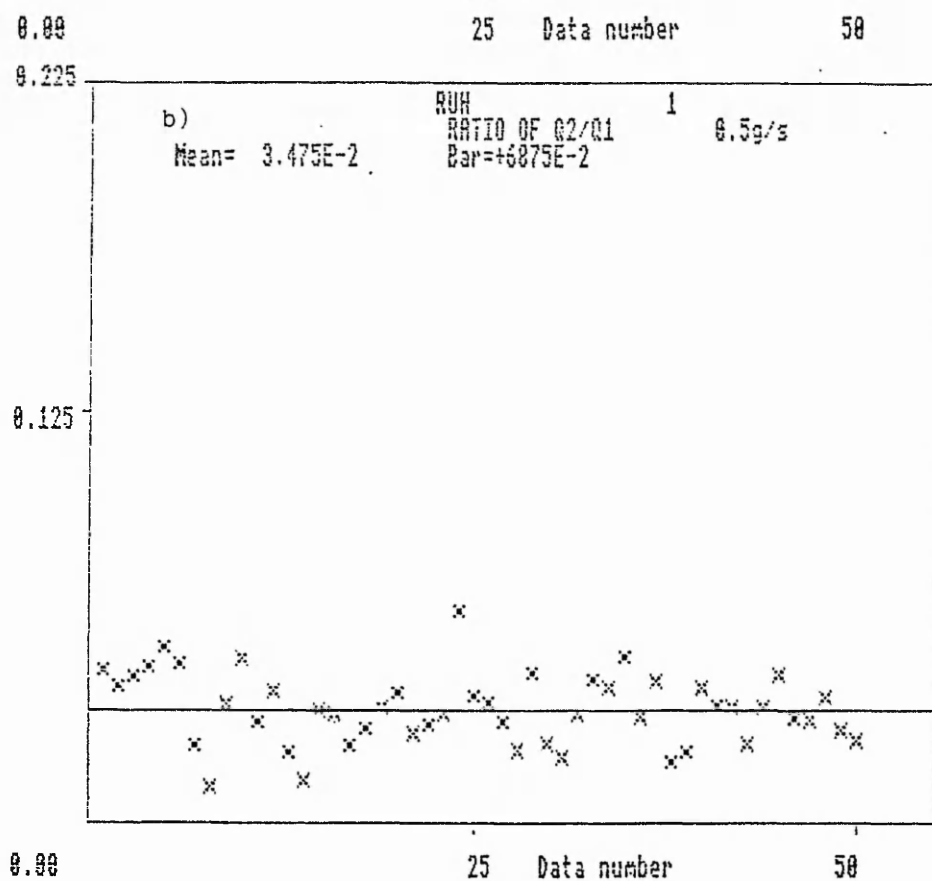
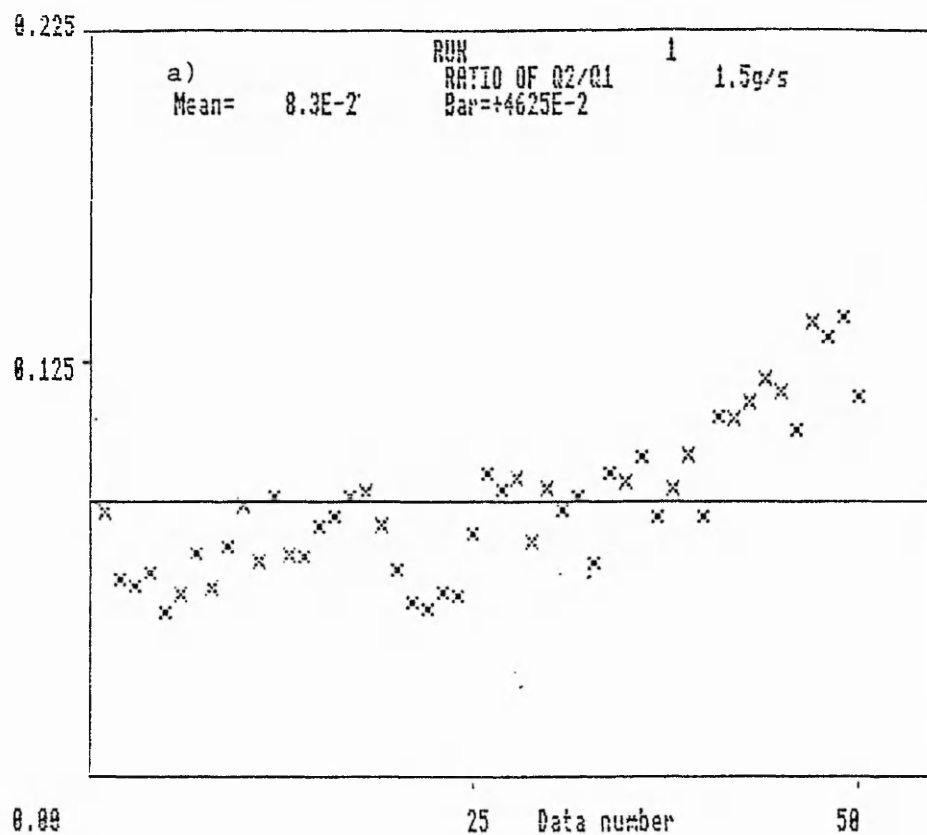


Fig 5.5

Data processing, error bar and mean value of Q2/Q1

5.5 Comparison With C.Willis[1]

The work of C.Willis[1] is based on current measurements, and the use of I_2/I_{inj} . The measurements used are peak to peak values, which makes the ratios I_3/I_2 , and I_4/I_3 possible to measure, in contrast to Q_3/Q_2 . The data processing consists of averaging the ratios in three regions of the flow, high, low and medium flow rates. The experiment uses a white epoxy/polyester powder. This type of powder is lighter than the one used here, and the flow rates discussed were in the order of 5.6 g/s. All the readings were taken manually hence averaging the data was a difficult task.

5.6 Conclusion

The aim of this analysis was to study the fluctuation of the flow, and the parameter used to predict the mass flow rate. The ratio Q_2/Q_1 is one of many parameters that are fairly proportional to the flow, and it seems to be stable especially at low flow rates.

Analysis based on standard deviation, shows that the ratio Q_2/Q_1 is linear within an error of + 5%. This may depend on the type of powder, but definitely not on the operating conditions such as the power supply voltage and pressure level.

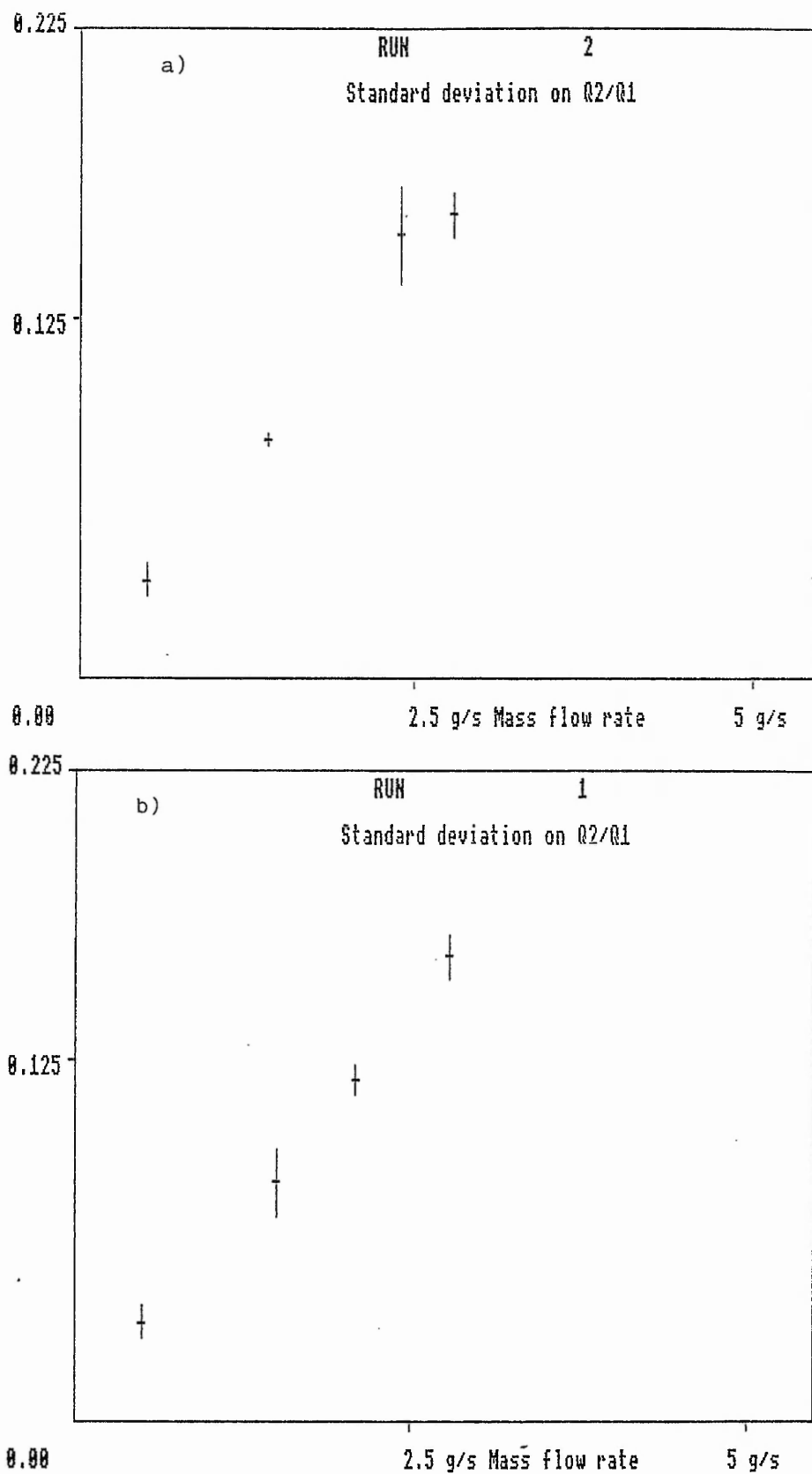


Fig 5.6

Data processing, standard deviation on the ratio $Q2/Q1$

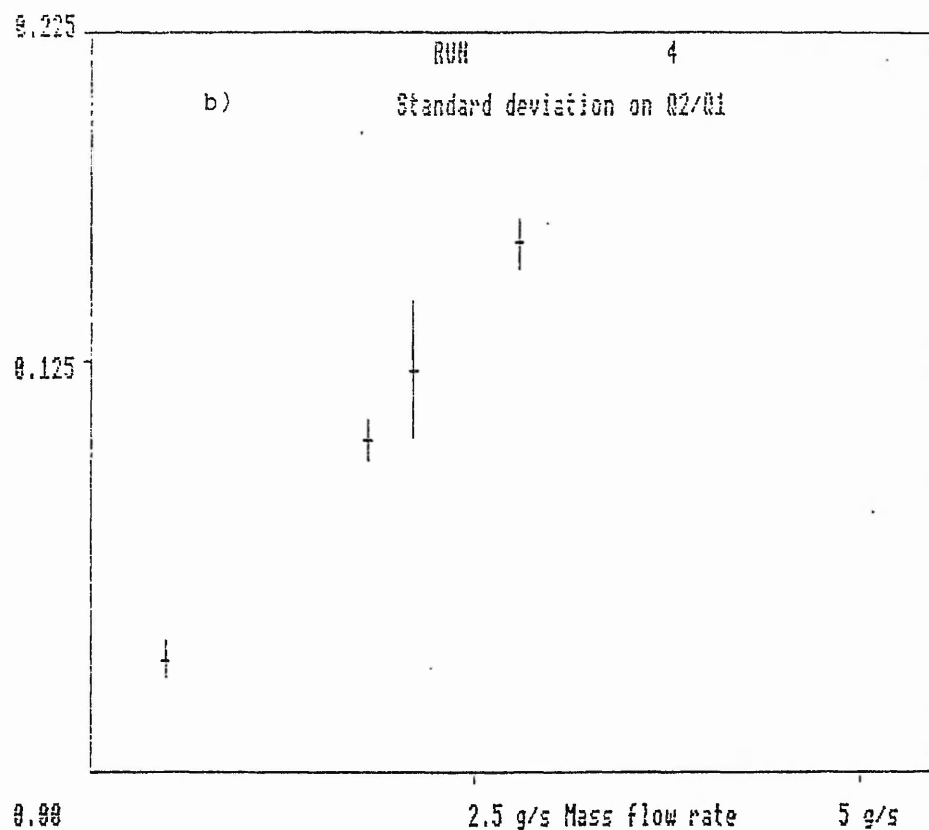
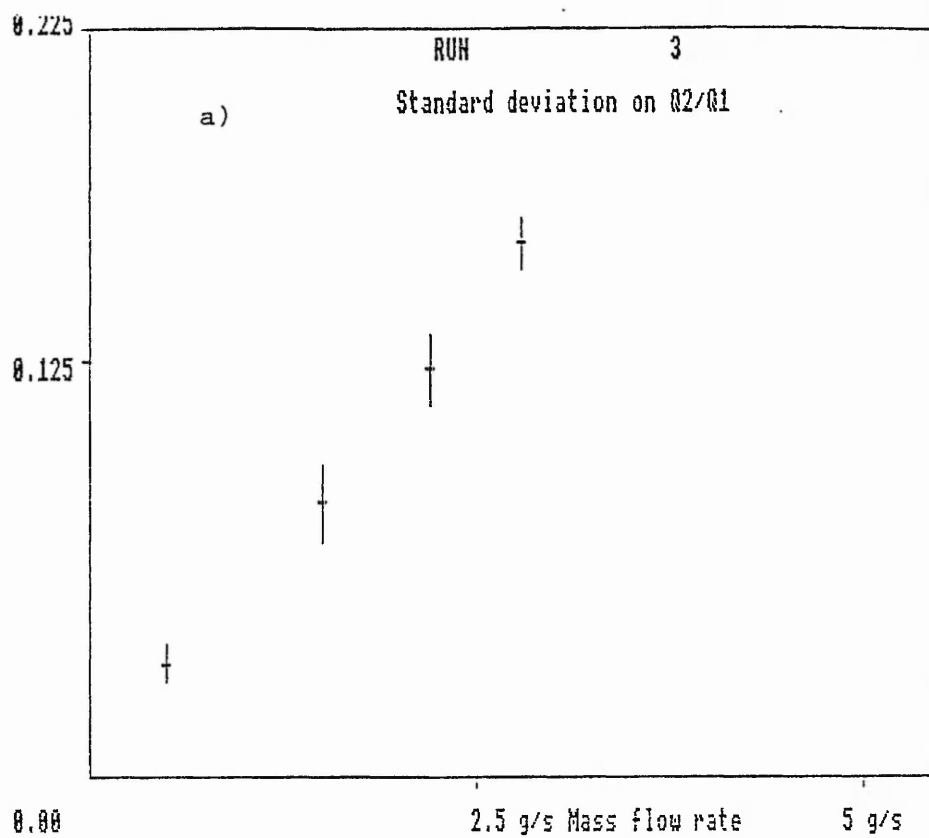


Fig 5.7

Data processing, standard deviation on the ratio Q2/Q1

Chapter 6

CONCLUSION AND FURTHER WORK

6.1 Conclusion

The project covered three parts which are the theory of charging and collection in electrostatic spraying, design of charge detection electronic instrument and the analysis of the parameters needed to predict the mass flow rate. First the theory of charged particles involves the study of the charge detection, with a variable sensor length and pulse width using Laplace's solution. Secondly the electronic instrument is designed to be of low noise and high accuracy, hence circuit analysis of the analog circuitry was needed. Finally the data analysis based on error bar and standard deviation was used to study the linearity of the parameters for mass flow rate prediction.

The theory of charged particles is more accurate than the previous one which used the assumption of parallel plates. The flux collected by a sensor length of 21mm and a pulse charge of 21mm is optimized to 85 % of the total flux. The instrument can measure a current of 0.1uA with an error of 5 %. The noise is found to be small, thus small errors are allowed when reading low charge values. The analysis shows that the parameter which is used to predict the mass flow rate, Q_2/Q_1 , is within an error of + 10 %.

The previous work might be optimized at its best performance when the following notes are fulfilled.

1- The theory of charged particles can be developed to include the flow parameter in order to simulate the charging process for a computer model. Although it is a difficult task because it involves the theory of turbulent flow.

t

2- The electronic instrument, which is the charge detection device, needs a noise reduction technique, and replacement of the sample and hold integrated circuits with faster ones

3- The present process for data analysis takes 10 minutes to read four channels each with 1000 samples. The processor cannot be accelerated because the pulse charge cycle time is 20 ms. This suggests a multichannel use where a processor is connected to several systems.

6.2 Further work

For future work the electrostatic spraying incorporating the pulse charge injection measurement technique, should be fully controlled and computerised. It appears that two topics may contribute to the improvement of the electrostatic spraying performance. These are the high voltage power supply and the control of the flow process.

The power supply presents problems during the charging of the powder, which affects the measurement of the flow, and the safety of the process. The flow of the powder is not uniform due to a critical parameter which might lead to a poor quality of the coated surface. Flow control is needed to try and stabilise the flow.

6.2.1 High voltage pulse generator.

The actual power supply used in the experiment is a commercial high voltage pulse generator, which has a complex internal structure to provide switching of the high voltage giving a sharp response. For industrial use it is important to have a power supply that is easy to build, cheap and more reliable, providing it can still fulfill the previous requirement of switching.

At the beginning, the project includes a design of a new power supply, which can deliver higher voltage level, †

which enable the powder to be discharged, and a power supply that might interface with the computer for control purpose. †

6.2.2 Powder flow control

The flow control depends on many parameters. The major parameters are particle size and particle resistivity. Good quality powder coating depends on the uniformity of the flow. Since this is currently not available, a good flow control process is needed to try and give this uniformity.

At the end of this project it was suggested to initialise a basic idea of flow control. The flow chart in Fig 6.1 presents the idea. This consists of measuring the parameter that predicts the flow rate. The next step is to control the flow by driving the valves of the pneumatic system using a stepper motor. Due to the lack of time this was not completed.

Mass flow rate control work carried out, used a SYNTTEL 6809 development system. The software was written with the full development tools of the system, unlike the 6502 programming on the BBC which had no development tools. The software is based on the principle of measuring the average ratio $Q2/Q1$ and comparing it to the reference value, adjusting the flow up or down according to the result. The reference value is a variable potential, read by the ADC. The hardware contains an 8-bit 4-channel A/D converter, a stepper motor drive I.C and a PIA. Port A of the PIA is used as input from the ADC, and port B as output to the stepper motor drive to set the number of turns and the direction. The hardware is implemented on a eurocard which interfaces to the external bus of the SYNTTEL system.

The software representing the basic idea of flow control is outlined in appendix E.

2.2.3 Electrostatic precipitators

The process applied to electrostatic spraying, treated in chapter 2, assumes the flow to be high density. Further investigation into the low density region of the flow may be carried out to monitor electrostatic precipitators, which are used for gas cleaning. This is aimed to produce better complex analytical and computers models, and to optimise the precipitator's overall performance, mainly the collection of high resistivity particulates. The pulse charging mass flow measurement technique should be used as an important tool for this work.

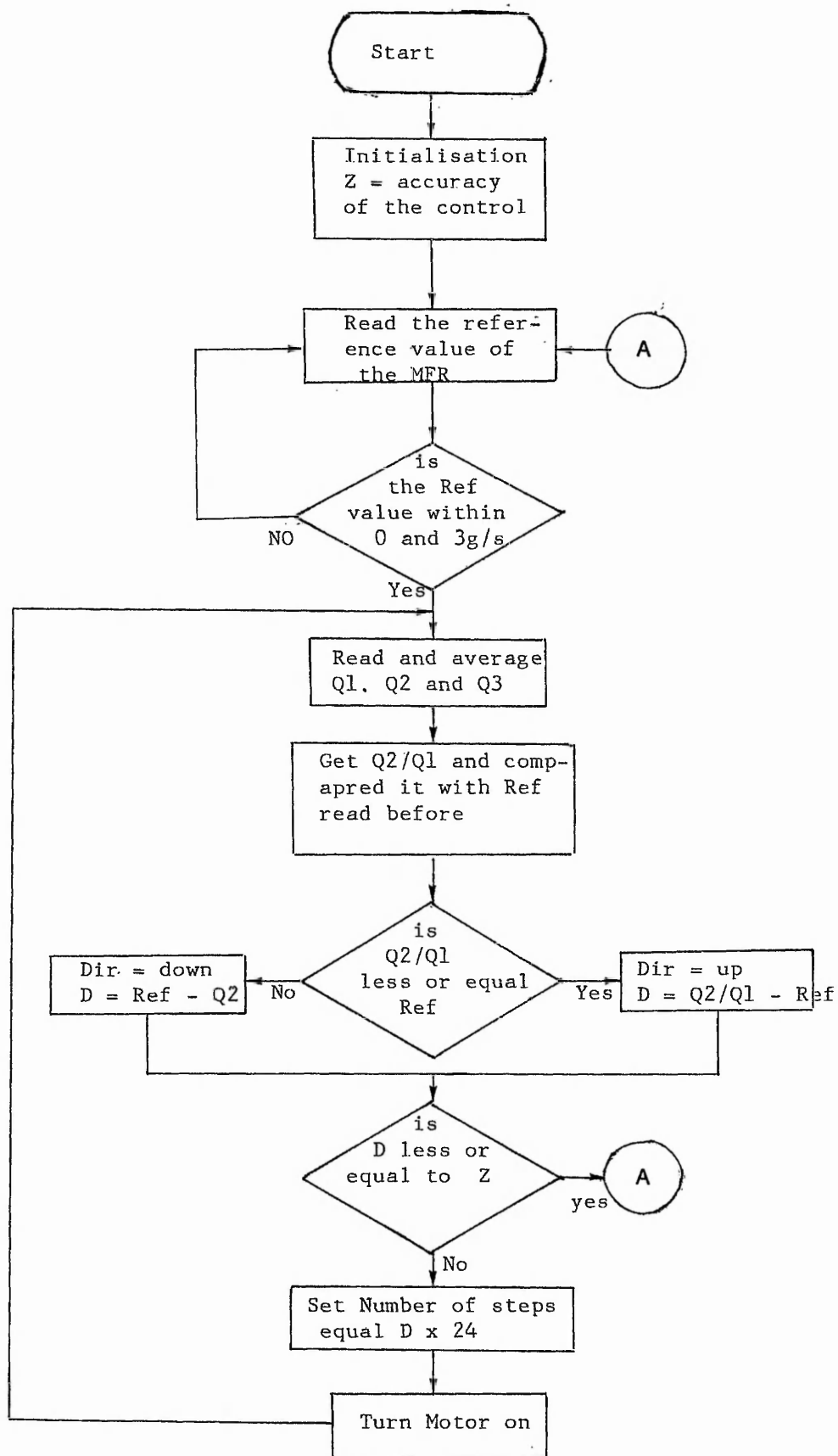


Fig 6.1

REFERENCES

- [1] B.C.O'Neill & C.A.Willis
"Corona discharging of pneumatically conveyed powders"
J.Electrostatics, EFCE, June 1985. Vol 17, n° 1, pp 99-108
- [2] R.G.Green & J.M.Cunliffe
"A frequency Modulated Capacitance Transducer for on
line Measurement of two Components Fluid flow"
Measurement, Vol 1, No 4, pp 191-195.
- [3] H.K.Kwan & M.S.Beck
"Mass Flow Measurement of Solid in Gravity Conveyors
using Capacitance and Ultrasonic Transducers"
Proc, 7th IMEKO conf, prac, meas, pp 375-80, 1976.
- [4] G.N.Malyshev
"Equipment for Measuring the Delivery of coal dust
feed" IXV, VUZ, Energy, USSR, June 1981, no 6, pp 118-20.
- [5] C.A.Willis & B.C.O'Neill
"Pneumatic conveyed Continuous Mass Flow Rate"
Ph.D 1985.
- [6] W.K.H.Panofsky & M.Philips
"Classical Electricity and Magnetism"
Addison-Wesley, Reading, Mass 1955, pp 48-80.
- [7] A.D.Moore
"Electrostatics & its applications"
Wiley-Interscience, N.Y
- [8] P.Lorrain & D.Corson
"Electromagnetic fields and waves"
W.H.Freeman company, pp 168-80.
- [9] Martin & A.Plonus
"Applied Electromagnetics" chap 2.
McGraw-Hill Kogakusha, ltd.
- [10] M.D.R Beasley & DR Picklers
"Comparative study of three Methods for Computing Electric
Fields" Proc, IEE Jan 1979, Vol 126, No 1, pp 126-43.
- [11] J.Deuse et J.L.Lilien
"Les methodes de calcul Numerique des Champs Electriques
leurs possibilites et leurs limitations", pp 203-213.
Electrotech, Montefiore, belgium 1977, Vol 90.

- [12] G.B.Clayton
"Operational amplifier" Butter Worth & Co.
- [13] J.Millman & C.C.Halkis
"Intergrated cercuit" McGraw-Hill Kogakusha, ltd.
- [14] Horowitz & Hill
"The art of Electronics" Cambridge university press.
- [15] Ambrozy
"Electronic noise" chap 8, McGraw-Hill International book.
- [16] T.H.Wilmshurst
"Signal recovery form noise in Electronic instrumentation"
Adam Hilger, ltd. Bristol, Bost.
- [17] K.H.Abdul-Hameed & M.A.Abdul-Karim
"Signal processing circuit for mass flow rate digital
meter design" Rev, Sci, Instrum, July 1987, Vol 58, No 7
pp 1242-45
- [18] BBC user manual. Cambridge company.
- [19] BBC advanced manual. Cambridge company.
- [20] D.Peritty
"Practical Interface to Popular Microprocessors", chap 10
Addison-Wesley publishing company.
- [21] Marvin & L.De Jong
"Programing and interfacing the 6502 with experiment"
Howard W.Sams & Co, Inc.
- [22] "The influence of Microelectronics on measurement
instrumentation Transducer Design" UMIST July 1982.
- [23] Robert SH.Habib & Qais A.H.Alnouman
"Microcomputer-based liquid flow rate control system"
INT.J.Electronics 1988, Vol 65, no 1, pp 117-125.
- [24] Prof J.R.Smith & D.McAllister
"Experimental and Numerical Investigation on low
Conductivity Powder Transport" IEE 1983, Vol 130, pt 4
no 7, pp 369-380.
- [25] "Industrial Course in Electrostatics Coatings"
Powders and paints". Semp 1976, Southampton university.
- [26] "International conference of Mass flow Measurement
in mid 80's". June 1986, Glasgow, volume 1,2 . Int, Eng, Lab
- [27] J.R.Jordan
"Correlation, algorithms, circuits and measurements

[27] J.R.Jordan

"Correlation, algorithms, circuits and measurement
applications" IEE proceedings, February 1986

[28] K.J.McLean

"Electrostatic Precipitators"
IEE Review July 1988

APPENDIX A

The solution of a point charge inside a grounded conducting cylinder is not an easy problem to solve since the potential is function of three variables.

Laplace's equation in cylindrical coordinates is:

$$\frac{1}{r} \frac{\partial}{\partial r} \left(r \frac{\partial \Psi}{\partial r} \right) + \frac{1}{r^2} \frac{\partial^2 \Psi}{\partial \phi^2} + \frac{\partial^2 \Psi}{\partial z^2} = 0 \quad (\text{A-1})$$

The separation of the potential function by means of a product. lead to

$$\Psi(r, \phi, z) = R(r) \cdot \Theta(\phi) \cdot Z(z) \quad (\text{A-2})$$

Putting (A-1) in (A-2) gives:

$$r \frac{d}{dr} \left(r \frac{dR}{dr} \right) + (k^2 r^2 - n^2) R = 0 \quad (\text{A-3})$$

$$\frac{d^2 \Theta}{d\phi^2} + n^2 \Theta = 0 \quad (\text{A-4})$$

$$\frac{d^2 Z}{dz^2} - k^2 Z = 0 \quad (\text{A-5})$$

Where n , and k are the separation parameters. (A-3) is known as Bessel equation, and its solutions are called Bessel function. Because of the symmetry of the cylinder, the potential is independent on the angle ϕ , so $n = 0$, and $\Theta = \text{constant}$.

The solution of (A-3) and (A-5) are respectively:

$$Z = E_k \exp(k z) + F_k \exp(-k z) \quad (\text{A-6})$$

$$R = A_k J_0(k r) \quad (\text{A-7})$$

Equation (A-2) could be written as:

$$\Psi_1 = \sum_1 A_1 J_0(k_1 r) \exp(-k_1 z) \quad , \quad z > 0 \quad (\text{A-8})$$

$$\Psi_2 = \sum_1 A_1 J_0(k_1 r) \exp(k_1 z) \quad , \quad z < 0 \quad (\text{A-9})$$

Because the walls are grounded this means that $\Psi(r_0) = 0$, thus $J_0(k_1 r) = 0$, k_1 are defined as the ensemble of solutions. The surface density of charge is $\sigma(r) = q \delta(r)$, where $\delta(r)$ is a two dimensional density of distribution, defined as

$$2\pi \int_0^{r_0} \delta(r) r dr = 1 \quad (\text{A-10})$$

The potential should satisfy the expression

$$\nabla^2 \Psi = - \frac{\rho}{\epsilon_0} \quad (\text{A-11}) \quad *$$

The first term of (A-11) can be written as

$$\nabla^2 \Psi = - \frac{\partial}{\partial z} \left(\frac{\partial \Psi}{\partial z} \right) = \left[\frac{\partial \Psi}{\partial z} (z^+) - \frac{\partial \Psi}{\partial z} (z^-) \right]_{z=0} \quad (\text{A-12})$$

Hence

$$\frac{\sigma(r)}{\epsilon_0} = \left[\frac{\partial \Psi_1}{\partial z} - \frac{\partial \Psi_2}{\partial z} \right]_{z=0} \quad (\text{A-13})$$

Using (A-8) and (A-9) it follows

$$q \frac{\delta(r)}{\epsilon_0} = 2 \sum_1 k_1 A_1 J_0(k_1 r) \quad (\text{A-14})$$

When multiplying both sides of (A-14) by $\int_0^{r_0} J_0(k_1' r) r dr$ this becomes

$$q \int_0^{r_0} J_0(k_1' r) \delta(r) r dr = 2 \sum_1 k_1 A_1 \int_0^{r_0} J_0(k_1' r) J_0(k_1 r) r dr \quad (\text{A-15})$$

$\delta(r)$ has one criteria defined as

$$2\pi \int_0^{r_0} f(r) r \delta(r) dr = f(0)$$

So the first term of (A-15) becomes equal to $q \frac{J_0(0)}{2\pi\epsilon_0}$. An other feature of Bessel function known as the orthogonality, defined as

$$\int_0^{r_0} J_0(k_1 r) J_0(k_1' r) dr = 0, \quad 1 \neq 1' \quad (\text{A-17})$$

Now using (A-17) the second term of (A-15) becomes equal to

$$2 k_1 A_1 [J_0(k_1 r)]^2 r dr \quad (A-18)$$

Putting (A-16) and (A-18) in (A-15) gives

$$A_1 = \frac{q}{2\pi \epsilon_0 k_1} \frac{J_0(0)}{\int_0^{r_0} \{ J_0(k_1 r) \}^2 r dr} \quad (A-19)$$

Bessel function derivation is known as

$$J_n'(x) = J_{n+1}(x) + \frac{n}{x} J_n(x)$$

The same here is

$$\int_0^{r_0} [J_0(k_1 r)]^2 r dr = \frac{r_0^2}{2} [J_1(k_1 r_0)]^2 \quad (A-20)$$

Finally putting (A-20) in (A-19) gives

$$A_1 = \frac{q}{2\pi \epsilon_0 k_1} \frac{1}{\{ J_1(k_1 r_0) \}^2 r_0^2} \quad (A-21)$$

Now the final form of (A-8) and (A-9) when replacing (A-21) in these is

$$\psi = \frac{q}{2\pi r_0^2 \epsilon_0} \sum_1 \exp(k_1 |z|) \frac{J_0(k_1 r)}{k_1 [J_1(k_1 r_0)]^2}$$

APPENDIX B

This appendix present a detailed circuit analyses of the current to voltage converter and the integrator treated in chapter three. The analyses here are based upon the input impedance and the input offset current of the current to voltage converter, and the integrator drift.

B-1 current to voltage converter.

a) Input impedance: The circuit of Fig B-1 present a real current to voltage converter, which uses a real op-amp.

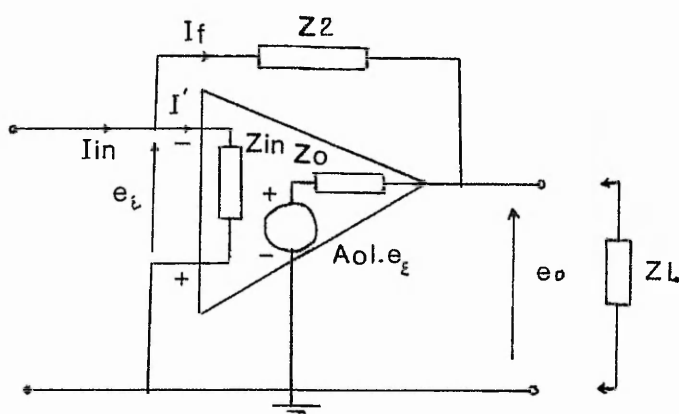


Fig B-1

From the circuit above it follows that:

$$I' = e_i / Z_{in} \quad (B-1)$$

And

$$I_f = (e_i - e_o) / Z_2 \quad (B-2)$$

Also

$$I_{in} = I' + I_f \quad (B-3)$$

Now substituting (B-1) and (B-2) in (B-3) gives:

$$I_{in} = (e_i / Z_{in}) + (e_i - e_o) / Z_2 \quad (B-4)$$

Usually $Z_L \gg Z_o$ hence, $e_o = -A_{ol}.e_o$. Equation (B-4) becomes

$$I_{in} = e [(1 / Z_{in}) + (1 + A_{ol}) / Z_2] \quad (B-5)$$

An ideal op-amp has an open loop gain A_{ol} infinit which means that the last term of (B-5) is infinit and the first term is nil, which make the input impedance infinit. Finally the input impedance of a real current to voltage converter is

$$1/Z_{in1} = [1/Z_{in1} + (1 + A_{ol}(w))/Z_2]$$

b) input offset current: The circuit of Fig (B-2) show the offset currents at both input terminals of a real op-amp. Where V_{io} is the input offset voltage, I_b^+ and I_b^- are the input bias current.

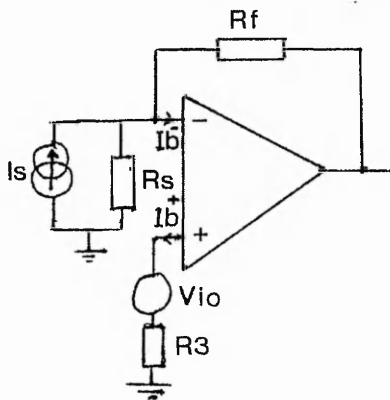


Fig B-2

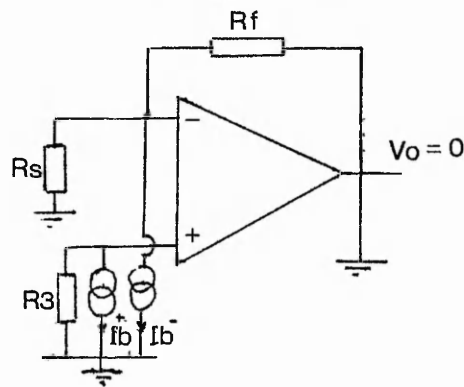


Fig B-3

When measuring the total offset voltage E_{os} , the output V_o should equal to zero, which bring R_f in parallel with R_s in Fig B-3. The equivalent circuit of this is in Fig B-4. The total offset voltage is:

$$E_{os} = (R_f // R_s) \cdot I_b^- - R_3 \cdot I_b^+ + V_{io}$$

E_{os} is minimum when $R_3 = (R_f // R_s)$, the above equation may be written as

$$E_{os} = (R_3 // R_f) \cdot I_{io} + V_{io}$$

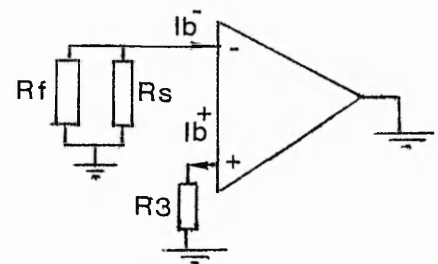


Fig B-4

Where $I_{io} = (I_b^- - I_b^+)$ is the input offset current.

The output offset voltage is equal to (E_{os}/β) , where β is the feedback fraction $\beta = R_s / (R_s + R_f)$. the output offset current is

$$I_{os} = E_{os} / (\beta \cdot R_f)$$

Finally

$$I_{os} = + V_{io} / (R_f // R_s) + I_{io}$$

B-2 Integrator:

A real integrator is shown below in Fig B-5

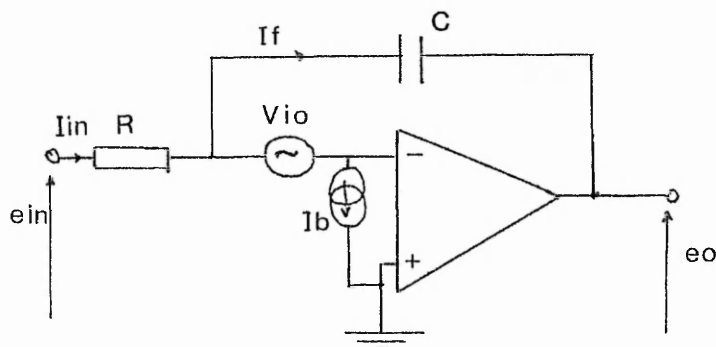


Fig B-5

Where V_{io} : the input offset voltage

V_c : the voltage across the capacitor

I_b : the input bias current

I_f : the feedback current.

If the open loop gain and the input impedance of the op-amp are infinite, it follows that:

$$I_{in} = I_f + I_b \quad (B-10)$$

And

$$I_{in} = (e_{in} \pm V_{io}) / R \quad (B-11)$$

Also

$$V_c = \pm V_{io} - e_o = \int \frac{I_f}{C} dt \quad (B-12)$$

Now using (B-11) in (B-12)

$$V_c = \frac{1}{C} \int (I_{in} - I_b) dt \quad (B-13)$$

Again using (B-11) in (B-12)

$$V_c = \int \frac{e_{in}}{RC} dt \pm \int \frac{V_{io}}{RC} dt - \frac{1}{C} \int I_b dt \quad (B-14)$$

Finally using (B-12) gives:

$$e_o = - \int \frac{e_{in}}{RC} dt \pm \int \frac{V_{io}}{RC} dt + \frac{1}{C} \int I_b dt \pm V_{io} \quad (B-15)$$

APPENDIX C

Electric feild and electric flux density programs in FORTRAN. This appendix contains five files as :

- 1- BESSEL.FOR
- 2- ELECL.FOR
- 3- ELECP.FOR
- 4- DENSL.FOR
- 5- DENSP.FOR

BESSEL.FOR is a program that find bessell function solution $J_0(a)=0$, which uses a numerical solution.

```
$ ty besse1.for
C   BESSEL FUNCTION PROGRAM
C   SOLUTIONS OF  $J_0$ 
C   ...FUNCTION REFERENCES...
C   REAL S17AFE,S17AEE
C   ...TABLE OF SOLUTION...
C   REAL IALPHA,A
10  FORMAT(1H,T20,'The solution of' bessell function  $J_0$  is')
20  FORMAT(1H0,T12,'Solution number',T38,'A value',T54,' $J_1$ ')
30  FORMAT(' ',T12,I3,T35,1PE12.3,T49,2F10.3,T60,1PE12.5)
    WRITE(6,10)
    WRITE(6,20)
    A=0.0
    SUM1=0.0
    I=0.0
50  A=A+3.15
    I=I+1
    R=10E-05
40  IFAIL=1
    V=S17AEE(A,IFAIL)
    P=ABS(V)
    IF (P.LE.R) THEN
        V1=S17AFE(A,IFAIL)
        SUM1=SUM1+1/(A*V1)
        WRITE(6,30) I,A,V1,SUM1
        GOTO 50
    ELSE
        A=A-P
        GOTO 40
    ENDIF
END
```

ELECL.FOR is a program which find the electric feild due to a line charge induced at the walls of the pipe.

```

$ ty elecl.for
C    ELECTRIC FEILD PROGRAM
C    CASE OF A LINE CHARGE
C    ...FUNCTION REFERENCES...
C    REAL S17AFE,S17AEE
C    ...TABLE OF SOLUTION...
C    DIMENSION X(140),Y(140)
C    ...Z/Ro=B...
C    ...L/2*Ro=CP...
REAL A,D1,D2,SUM1,SUM2,CS,CP
CALL PAPER(1)
CALL MAP(-3.00,3.00,0.00,0.80)
CALL AXES
CP=0.01
DO 75 J=1,4
WRITE(6,*)CP
  B=-3.0
  DO 70 K=1,140
    IF (ABS(B).LE.2E-02.OR.CP.GT.0.1) THEN
      P10=5E-03
    ELSE
      P10=1E-03
    ENDIF
    A=0.0
    I=0.0
    D2=10.0
    SUM1=0.0
50    A=A+3.40
    I=I+1
    R=10E-05
40    IFAIL=1
    V=S17AEE(A,IFAIL)
    P=ABS(V)
    IF (P.LE.R) THEN
      Z=S17AFE(A,IFAIL)
      R1=EXP(A*(CP-ABS(B)))
      R2=EXP(-A*(ABS(B)+CP))
      R3=EXP(-A*(CP-B))
      R4=EXP(-A*(CP+B))
      R5=2*Z*A*CP
      IF (ABS(B).LE.CP) THEN
        SUM2=SUM1+(2-(R3+R4))/R5
      ELSE
        SUM2=SUM1+(R1-R2)/R5
      ENDIF
      D1=ABS(SUM1-SUM2)
      IF (ABS(D1-D2).LE.P10) THEN
        SUM1=MIN(SUM1,SUM2)+D1/2
      ELSE
        SUM1=SUM2
        D2=D1
        GOTO 50
      ENDIF
    
```

```

ELSE
  A=A-F
  GOTO 40
ENDIF
X(K)=B
Y(K)=SUM1
WRITE(6,*)B,SUM1,K
  IF (ABS(B).LE.0.5) THEN
    B=B+0.01
  ELSE
    B=B+0.1
  ENDIF
70  CONTINUE
  CALL POSITN(X(1),Y(1))
  DO 100 IPT=2,140
    CALL JOIN(X(IPT),Y(IPT))
100  CONTINUE
    CP=CP+0.5
75  CONTINUE
  CALL PLOTCS(-1.00,0.80,'ELECTRIC FIELD SENSED AT THE WALLS')
  CALL PLOTCS(-0.50,0.75,'CASE OF A LINE CHARGE')
  CALL FRAME
  CALL GREND
  STOP
END

```

ELECP.FOR is a program which calculate the electric feild at the walls of the pipe, due to a point charge.

```
$ ty elecp.for
```

```

C      ELECTRIC FEILD PROGRAM
C      CASE OF A POINT CHARGE
C      ...FUNCTION REFERENCES...
      REAL S17AFE,S17AEE
C      ...TABLE OF SOLUTION...
      DIMENSION X(140),Y(140)
C      ...Z/Ro=B...
      REAL A,D1,D2,SUM1,SUM2,CS,CP
      B=-3.0
      DO 70 K=1,140
      IF (ABS(B).LE.10E-04) THEN
      X(K)=B
      Y(K)=0.663
      WRITE(6,*)X(K),Y(K)
      ELSE
      A=0.0
      I=0.0
      SUM1=0.0
      D2=10.0
50      A=A+3.15
      I=I+1
      R=10E-05
40      IFAIL=1
      V=S17AEE(A,IFAIL)
      P=ABS(V)
      IF (P.LE.R) THEN
      Z=S17AFE(A,IFAIL)
      SUM2=SUM1+EXP(-ABS(B)*A)/Z
      D1=ABS(SUM1-SUM2)
      IF (ABS(D1-D2).LE.1E-03) THEN
      SUM1=MIN(SUM1,SUM2)+D2/2
      ELSE
      D2=D1
      SUM1=SUM2
      GOTO 50
      ENDIF
      ELSE
      A=A-P
      GOTO 40
      ENDIF
      ENDIF
      IF (ABS(B).LE.0.5) THEN
      B=B+0.01
      ELSE
      B=B+0.1
      ENDIF
      X(K)=B
      X(K)=SUM1
      WRITE(6,*)B,SUM1,K

```

```

70  -- CONTINUE
    CALL PAPER(1)
    CALL MAP(-3.0,3.0,0.00,0.70)
    CALL AXES
    CALL POSITN(X(1),Y(1))
    DO 100 IPT=2,140
        CALL JOIN(X(IPT),Y(IPT))
100  CONTINUE
    CALL PLOTCS(-2.0,0.70,'ELECTIC FIELD SENSED AT THE WALLS')
    CALL PLOTCS(-1.0,0.70,'CASE OF A POINT CHARGE')
    CALL PLOTCS(1.00,0.025,'CYLINDER LENGTH /2*RADUIS (Z/2Ro)')
    CALL FRAME
    CALL GREND
    STOP
    END

```

DENSL.FOR is a program that find the electric flux density due to a line charge, at variable sensor and pulse length.

```
# ty densl.for
C   DENSITY OF CHARGE PROGRAM
C   CASE OF A LINE CHARGE
C   ...FUNCTION REFERENCES...
C   REAL S17AFE,S17AEE
C   ...TABLE OF SOLUTION...
C   DIMENSION X(100),Y(100)
C   ...Z/Ro=B...
C   ...S/2*Ro=CS...
C   ...L/2*Ro=CP...
C   REAL A,D1,D2,CS,CP,SUM1,SUM2
C   CALL PAPER(1)
C   CALL MAP(0.00,3.40,0.00,12.00)
C   CALL AXES
C   CP=0.01
90  IF (CP.LE.1.6) THEN
C     CS=0.0
C     WRITE(6,*) CP
C     DO 70 K=1,35
C       A=0.0
C       I=0.0
C       SUM1=0.0
C       D2=10.0
50    A=A+3.40
C       I=I+1
C       R=10E-05
40    IFAIL=1
C       V=S17AEE(A,IFAIL)
C       P=ABS(V)
C       IF (P.LE.R) THEN
C         Z=S17AFE(A,IFAIL)
C         R1=EXP(-A*ABS(CS-CP))
C         R2=EXP(-A*(CS+CP))
C         R3=1/(2*CP*A)
C         R4=CS/CP
C         IF (CS.LE.CP) THEN
C           SUM2=SUM1+20*(R4-R3*(R1-R2))/(Z*A)
C         ELSE
C           SUM2=SUM1+20*(1-R3*(R1-R2))/(Z*A)
C         ENDIF
C         D1=ABS(SUM1-SUM2)
C         IF (ABS(D1-D2).LE.10E-03) THEN
C           SUM1=MIN(SUM1,SUM2)+D1/2
C         ELSE
C           D2=D1
C           SUM1=SUM2
C           GOTO 50
C         ENDIF
C       ELSE
C         A=A-P
C         GOTO 40
C       ENDIF
C       X(K)=CS
C       Y(K)=SUM1
C       CS=CS+0.1
70  CONTINUE
```



```

ELSE
  GOTO 110
ENDIF
CALL POSITN(X(1),Y(1))
DO 100 IPT=2,35
  CALL JOIN(X(IPT),Y(IPT))
100 CONTINUE
CP=CP+0.5
GOTO 90
110 CALL PLOTCS(0.5,11.50,'Density of charge with respect ')
CALL PLOTCS(0.6,11.00,'to the sensor length')
CALL PLOTCS(0.5,10.50,'case of a line of charge')
CALL PLOTCS(1.00,0.25,'Sensor length /2*raduis (S/2Ro)')
CALL FRAME
CALL GREND
STOP
END

```

DENSP.FOR is program that find the electric flux density due to a point charge, at variable sensor length.

```

$ ty densp.for
C   DENSITY OF CHARGE PROGRAM
C   CASE OF A POINT CHARGE
C   ...FUNCTION REFERENCES...
C   REAL S17AFE,S17AEE
C   ...TABLE OF SOLUTION...
C   DIMENSION X(45),Y(45)
C   ...Z/Ro=B...
C   ...S/2*Ro=CS...
C   ...L/2*Ro=CP...
C   REAL A,D1,D2,CS,SUM1,SUM2
C   CS=0
C   DO 70 K=1,35
C   A=0.0
C   I=0.0
C   SUM1=0.00
C   D2=20.0
50  A=A+3.40
C   I=I+1
C   R=10E-05
40  IFAIL=1
C   V=S17AEE(A,IFAIL)
C   P=ABS(V)
C   IF (P.LE.R) THEN
C   Z=S17AFE(A,IFAIL)
C   SUM2=SUM1+20*(1-EXP(-A*CS))/(Z*A)
C   D1=ABS(SUM1-SUM2)
C   IF (ABS(D1-D2).LE.10E-03) THEN
C   SUM1=MIN(SUM1,SUM2)+D1/2
C   ELSE
C   D2=D1
C   SUM1=SUM2
C   GOTO 50
C   ENDIF
C   ELSE
C   A=A-P
C   GOTO 40
C   ENDIF
C   X(K)=CS
C   Y(K)=SUM1
C   WRITE(6,*) CS,SUM1
C   CS=CS+0.1
70  CONTINUE
C   CALL PAPER(1)
C   CALL MAP(0.00,3.50,0.00,11.00)
C   CALL AXES
C   CALL POSITN(X(1),Y(1))
C   DO 100 IPT=2,35
C   CALL JOIN(X(IPT),Y(IPT))
100 CONTINUE
C   CALL PLOTCS(0.40,11.00,'Density of charge with respect ')
C   CALL PLOTCS(0.50,10.50,'to the sensor length')
C   CALL FRAME
C   CALL BREND
C   STOP
C   END

```

APPENDIX D

Data processing, and main program of data record. This appendix contains three files as :

1- MAIN.BAS

2- ERR.BAS

3- DEV.BAS

MAIN.BAS is the main program which collect the data.

```
10 DIM A%(100),B%(100),C%(100)
20 REM The program trigger th power
30 REM supply, and record 100 avereges
40 REM of three channels each average
50 REM is of 10 readings
60 REM then save the data in a file
100 PROCadc
130 CALL reset
140 CALL avrge
145 FOR I=0 TO 99 STEP 2
150 A%(I)=?(&2A00+I)+256*?(&2A01+I)
160 B%(I)=?(&2B00+I)+256*?(&2B01+I)
170 C%(I)=?(&2C00+I)+256*?(&2C01+I)
180 PRINT A%(I),B%(I),C%(I)
190 NEXT
200 PROCstore
210 END
2000 DEFPROCadc
2005 CONF=&80
2010 AVRG=&10
2015 CHNL=&20
2120 DIM M% 250
2130 FOR opt%=0 TO 2 STEP 2
2140 P%=M%
2150 [
2160 OPT opt%
2170 \
2180 \ START ROUTINE \
2190 \
2200 .avrge LDA &10 \ set mem &10 with
2210 STA AVRG \ 10 ten readings
2220 .start LDA &4
2230 STA CONF
2240 LDA &2A
2250 STA &73
2260 LDA &3
2270 STA CHNL
2290 LDA &80 \ trigger power
2300 STA &FE62 \ supply
2303 STA &FE60
2305 LDA &0
2307 STA &FE60
2310 JSR delay \ wait 12ms
2320 .next JSR ADC
2330 JSR add
2340 INC CONF
2345 DEC CHNL
2350 BNE next \ make an average
2351 DEC AVRG \ of 10 values
2353 BNE start
2355 INC &72 \ make 100 average
2357 INC &72 \ each time take
2359 BNE avrge \ two bytes
```

```

2361          RTS
2363 \
2365          \ A TO D ROUTINE \
2367 \
2370 .ADC      LDA &F \ set first 4 bits
2380          STA &FE62 \ as output
2390          SEI
2400          LDA &FE6C \ CB2 low ,R/W
2410          AND &1 \ CA2 high ,DIR,RD
2420          ORA &CE \ interrupt,CB1
2430          STA &FE6C \
2440          LDA &FE60 \ clear input re
2450          AND &0
2460          ORA CONF \ set config of
2470          STA &FE60 \ multiplexer
2480          LDA &FE6C
2490          ORA &20
2500          STA &FE6C \ stat convers
2510          CLI
2530          LDA &FE6D \ is interr set
2540          AND &90
2550          CMP &90
2560          BNE exit
2570          STA &FE6D \ clear interrup
2590 .exit     LDA &FE6C
2600          AND &FD \ CB2 as high and
2610          STA &FE6C \ CA2 as low.
2765          RTS
3000 \
3010          \ CLEAR ROUTINE \
3020 \
3030 .reset    LDA &2A \ clear 3 pages
3040          STA &73 \ of memory from
3050          LDX &3 \ 2A00 to 2C00
3060          LDA &0
3070          STA &72
3080          LDY &0
3090          LDA &0
3100 .loop     STA (&72),Y
3110          INY
3120          BNE loop
3130          INC &73
3140          DEX
3150          BNE loop
3160          RTS
4000 \
4010          \ DELAY ROUTINE \
4020 \
4030 .delay    LDX &A \ delay of 12ms
4040 .DLY2     LDY &0
4050 .DLY1     DEY
4060          BNE DLY1
4070          DEX
4080          BNE DLY2
4090          RTS
4100 \
4110          \ ADDITION ROUTINE \
4120 \
4125 .add      LDA &0 \ all inputs

```

```

4130      STA &FE62
4135      LDA &FE60
4140      CLC
4150      ADC (&72),Y \ add to the
4160      STA (&72),Y \ previous val
4170      INY          \ in 1 byte
4180      LDA &0
4190      ADC (&72),Y \ store carry
4200      STA (&72),Y \ in the 2 byt
4210      INC &73
4220      DEY
4310      RTS
4900 ]
4910 NEXT
5000 ENDPROC
5010 DEFPROCstore
5020 E%=OPENOUT"DATA"
5030 FOR I=0 TO 99 STEP 2
5040 PRINT$ E%,A%(I),B%(I),C%(I)
5050 NEXT
5060 CLOSE$E%
5070 ENDPROC

```

>

ERR.BAS is the program which find the error bar of the data af:each run.

Mistake

>L.

```
10 MODE3 :DIM DV(150)
20 DIM AV(150),BV(150)
25 DIM CV(150),M(150)
30 PROC_ASSEMBLE
70 E%=OPENIN"DAT0.5"
75 FOR I=1 TO 50
80 INPUT& E%,AV(I),BV(I),CV(I),M(I)
85 NEXT
86 CLOSE& E%
87 E%=OPENIN"DAT2.3"
88 FOR I=51 TO 100
89 INPUT& E%,AV(I),BV(I),CV(I),M(I)
90 NEXT
100 CLOSE& E%
101 E%=OPENIN"DAT2.8"
102 FOR I=101 TO 150
103 INPUT& E%,AV(I),BV(I),CV(I),M(I)
104 NEXT
105 CLOSE& E%
120 FOR I=1 TO 150
130 DV(I)=400*BV(I)/AV(I)
140 NEXT
181 PRINT "ENTER RUN NUMBER"
182 INPUT RNB
183 PRINT "ENTER MASS FLOW RATE"
184 INPUT MFR
185 MODE0
224 PROCdraw(7,7,51,100)
235 MN%=Mean
300 PROCbarr
445 MOVE 1200,100:DRAW 1100,100
450 MOVE 1100,90 :DRAW 1100,100
460 DRAW 600,100 :DRAW 600,90
470 MOVE 600,100 :DRAW 100,100
480 DRAW 100,600 :DRAW 90,600
490 MOVE 100,600 :DRAW 100,1000
495 DRAW 90,1000 :DRAW 1200,1000
500 DRAW 1200,100:MOVE 100,(100+Mean)
505 DRAW 1200,(100+Mean)
510 PRINT TAB(67,30) "100"
520 PRINT TAB(0,30) "0.00"
530 PRINT TAB(0,13) "0.125"
535 PRINT TAB(13,3)"Mean="
536 PRINT TAB(18,3)MN%/4E+3
540 PRINT TAB(0,0) "0.225"
550 PRINT TAB(37,30) "50"
560 PRINT TAB(43,30) "Data number "
580 PRINT TAB(35,2) "RATIO OF Q2/Q1"
581 PRINT TAB(50,2) MFR
582 PRINT TAB(60,2) "g/s"
590 PRINT TAB(34,1) "RUN",RNB
595 PRINT TAB(37,3) BARR
597 PRINT TAB(35,3) "Bar=+"
599 INPUT AS
600 IF AS=0 GOTO 605
```

```

603 CALL DUMP
605 END
610 DEFPROCbarr
620 MAX=0
630 MIN=1000
640 FOR J=1 TO 50
650 D1=DV(J)-MAX
660 D2=MIN-DV(J)
680 IF D1>0 THEN MAX=DV(J)
690 IF D2>0 THEN MIN=DV(J)
695 NEXT
696 BAR%=(MAX-MIN)
697 BARR=BAR%/8000
700 ENDPROC
800 DEFPROCdraw(Z,W,M,L)
805 Mean=0
810 FOR K=M TO L
815 X=2*M(K)+100:Y=DV(K)+100
820 MOVE X-Z,Y+W
830 DRAW X+Z,Y-W
840 MOVE X+W,Y+Z

850 DRAW X-W,Y-Z
870 Mean=Mean+DV(K)/50
880 NEXT
890 ENDPROC

```

>

DEV.BAS is the program which find the standard deviation of each run.

>L.

```
10 MODE3
15 PROC_ASSEMBLE
20 DIM AV(50),BV(50)
25 DIM RC(50),M(50)
30 DIM DEV(5),MEN(5)
70 E%=OPENIN"DAT0.5"
75 FOR I=1 TO 50
80 INPUT& E%,AV(I),BV(I),RC(I),M(I)
81 NEXT
85 PROCmean(1,1,50)
86 CLOSE& E%
87 E%=OPENIN"DAT1.5"
88 FOR I=1 TO 50
89 INPUT& E%,AV(I),BV(I),RC(I),M(I)
90 NEXT
95 PROCmean(2,1,50)
100 CLOSE& E%
101 E%=OPENIN"DAT2.3"
102 FOR I=1 TO 50
103 INPUT& E%,AV(I),BV(I),RC(I),M(I)
104 NEXT
105 PROCmean(3,1,50)
110 CLOSE& E%
120 E%=OPENIN"DAT2.8"
130 FOR I=1 TO 50
140 INPUT& E%,AV(I),BV(I),RC(I),M(I)
145 NEXT
146 PROCmean(4,1,50)
147 CLOSE& E%
150 PRINT "ENTER MFR : A,B,C,D"
151 INPUT M(1),M(2),M(3),M(4)
181 PRINT "ENTER RUN NUMBER"
182 INPUT RNB
185 MODE0
400 PROCdraw
445 MOVE 1200,100:DRAW 1100,100
450 MOVE 1100,90 :DRAW 1100,100
460 DRAW 600,100 :DRAW 600,90
470 MOVE 600,100 :DRAW 100,100
480 DRAW 100,600 :DRAW 90,600
490 MOVE 100,600 :DRAW 100,1000
495 DRAW 90,1000 :DRAW 1200,1000
500 DRAW 1200,100
510 PRINT TAB(67,30) "5 g/s"
520 PRINT TAB(0,30) "0.00"
530 PRINT TAB(0,13) "0.125"
540 PRINT TAB(0,0) "0.225"
550 PRINT TAB(37,30) "2.5 g/s"
560 PRINT TAB(45,30) "Mass flow rate"
580 PRINT TAB(31,3) "Standard deviation on Q2/Q1"
590 PRINT TAB(34,1) "RUN",RNB
600 CALL DUMP
605 END
805 DEFPROCdraw
```

```

810 FOR K=1 TO 4
815 X=M(K)*200+100:Y=MEN(K)+100
820 MOVE X-5,Y
830 DRAW X+5,Y
840 MOVE X,Y+DEV(K)/2
850 DRAW X,Y-DEV(K)/2
880 NEXT
890 ENDPROC
900 DEFPROCmean(Z,M,L)
905 MEAN=0
910 FOR I=M TO L
920 RC(I)=400*BV(I)/AV(I)
930 MEAN=MEAN+RC(I)/50
940 NEXT
950 MEN(Z)=MEAN
960 D3=0
970 FOR I=M TO L
980 D4=(MEN(Z)- RC(I))
990 D3=D3+D4^2
1000 NEXT
1010 DEV%=SQR(D3/50)
1020 DEV(Z)=DEV%
1030 ENDPROC

```

APPENDIX E

This software is the basic idea of flow regularisation explained in chapter 6.

```
NAM MAIN
TTL MAIN PROGRAM OF MFR CONTROL
IFP1
USE /D0/DEFS/OS9DEFS
ENDC
* MODULE HEADER DEFINITION
MOD PRGML,NAME,$11,$81,ENTER,MEMSZ
NAME FCS "MAIN"
* DATA EREA
RMB 3 work erea,calculations
Q1 RMB 20 data erea of the charges
Q2 RMB 20 Q1 and Q2 sensed
DIFF RMB 2
BITS RMB 1
NBPULS RMB 2
RATIO RMB 2 Q2/Q1
MFR RMB 2 reference mass flow rate
BLGTH RMB 1
RMB 256
RMB 200
MEMSZ EQU . MEMORY SIZE
* SYMBOLS DEFINITION
PIA EQU $C1B8 pia port 2
* PIA+2 port 3
* PROGRAM EREA
ENTER EQU *
*** P.I.A INITIALISATION ***
LDA #%00000000 SET DDRGA
STA PIA+1
LDA #$FF ALL OUTPUTS port 2
STA PIA
ORA #%00100100 SET DREGA
STA PIA+1
LDA #%00000000 SET DDRGB port3
STA PIA+3
LDA #$00 ALL INPUTS
STA PIA+2
ORA #%00100100 SET DREGB
STA PIA+3
ANDCC #$EF
*** READ ROUTINE ***
READ LEAX Q1,U clear previous data of Q1
LDB #20 ten data each of two bytes
LBSR CLEAR
LEAX Q2,U clear previous data of Q2
LDB #20 ten data each of two bytes
LBSR CLEAR
LDA #%00000011 set multiplexer
ORA PIA configuration
STA PIA for desired mass flow rate
LBSR ADC enter MFR
LDA WORK
STA MFR store MFR
```

```

AGAIN    LDB #20 load nbr of reading
        LDA #00000001 set config of ch1
        ORA PIA
        STA PIA
        BSR ADC read Q1
        LEAX Q1,U get previous value of Q1
        LDD ,X add it
        ADD ,U to the recent value
        STD Q1,U store it
        LDA #00000010 set multiplexer config
        ORA PIA for Q2
        STA PIA
        BSR ADC read Q2
        LEAX Q2,U get previous value of Q2
        LDD ,X add it
        ADD ,U to the recent value
        STD Q2,U store it
        DECB has record been completed
        BNE AGAIN if not branch to again
        LEAX Q1,U get add of Q1
        LEAY Q2,U get add of Q2
        BSR DIVDIT make division
        LDD ,U
        STA RATIO,U store it in ratio
        BSR MOTOR branch to motor routine
        CLRB
        OS9 F$EXIT
*** A to D CONV ROUTINE ***
ADC      LDA #00001000 set CB2 as high
        ORA PIA+3
        ANDA #11110111 set CB2 as low
        STA PIA+3
WAIT     LDA PIA+3
        CMPA #10110110
        BPL WAIT
        LDA PIA+2
        STA ,U
        RTS
*** STEPPER MOTOR ROUTINE ***
MOTOR    LDD MFR,U get MFR value
        CMPA RATIO,U compair with ratio Q2/Q1
        BCS DIRD branch to turn down
DIRU     LEAX MFR,U turn up if MFR is
        LDD ,X gretter than ratio
        SUBD RATIO,U substract ratio from
        STD DIFF,U MFR, store it in DIFF
        LDA #11110111 set turn up config
        ANDA PIA
        STA PIA
        BRA INPUT
DIRD     LEAX RATIO,U if ratio is gretter than MFR
        LDD ,X turn down,
        SUBD MFR,U substract MFR form ratio
        STD DIFF,U store it
        LDA #00001000 set turn down config
        ORA PIA
        STA PIA
INPUT    LDA DIFF,U
        CMPA #5 compair it to the accuracy
        BCS EXIT branch to exit if diff is
        LDB #24 less than the accuracy, multip
        MUL by 24 which is related to total nbr
        STD NBPULS,U of turns,

```

```

MORE      LDA #0
          ORA PIA
          STA PIA
          LBSR DELAY
          LDA #000000100
          ORA PIA
          STA PIA
          DEC NSPULS
          BNE MORE
          RTS

*** 16 BITS BY 16 DIVISION ROUTINE ***
DIVDIT    LDA #16 FOR 16 BIT DIVISION
          STA BITS,U
          LDA ,Y
          STA ,U
          LDA 1,Y
          STA 1,U
          CLRA
          CLRB
DVSIN     ASL 1,U SHIFT LEFT LSB
          ROL ,U ROTATE LEFT MSB
          ROLB
          ROLA
          CMPD ,X
          BLO NEXT
          SUBD ,X
          INC 1,U
NEXT      DEC BITS Y is the starting add of remaind
          BNE DVSIN
          STD REM,U store remainder
          RTS

*** CLEAR ROUTINE ***
CLEAR     CLR ,X+
          DECB
          BNE CLEAR
          RTS

*** DELAY ROUTINE ***
DELAY     LDX ##1250 10ms DELAY
          BRA DLY
DELAY1     LDX ##236 4.55ms DELAY
          BRA DLY
DELAY2     LDX ##5 40us DELAY
DLY        LEAX -1,X
          BNE DLY
          RTS

*** SUBSTACTION ROUTINE ****
*** 16 bit ADDITION ROUTINE ***
*** MOVE ROUTINE ***
MOVEDT    LDA ,X+      X:START ADDRESS OF DATA
          STA ,Y+      Y:FIRST ADDRESS WHERE TO MOVE DATA
          DECB         B:NUMBER OF BYTES TO BE MOVED
          BNE MOVEDT
          RTS
          CLRB
EXIT      OS9 F#EXIT
          EMOD
PRGML     EQU *

```